Article

Not peer-reviewed version

Techno-Economic Optimization of Hydrogen-Based Hybrid Renewable Energy Systems for Rural Electrification in Sub-Saharan Africa: Case Study of a Photovoltaic/Wind/Hydrogen System in Dargalla, Cameroon

Nasser Yimen * , Thierry Roger Mondoue Bouodo , Alain Christian Biboum , Urbain Nzotcha * , Bashir Musa , Rolland Djomi , Salisu Sani

Posted Date: 25 December 2024

doi: 10.20944/preprints202412.2206.v1

Keywords: hybrid renewable energy systems; hydrogen; fuel cell; electrolizer; sub-Saharan Africa; optimization; sensitivity analysis; solar photovoltaic (PV); Wind energy

Article

Techno-Economic Optimization of Hydrogen-Based Hybrid Renewable Energy Systems for Rural Electrification in Sub-Saharan Africa: Case Study of a Photovoltaic/Wind/Hydrogen System in Dargalla, Cameroon

Nasser Yimen [1,2,*], Thierry Roger Mondoue Bouodo [1], Alain Christian Biboum [1], Urbain Nzotcha [1], Bashir Musa [3], Rolland Djomi [1] and Sani Salisu [2]

[1] National Advanced School of Engineering, University of Yaoundé I, POB: 8390, Yaounde, Cameroon
[2] Department of Electrical Engineering, Ahmadu Bello University Zaria , Abuja, Nigeria
[3] Transmission Company of Nigeria (TCN), Plot 14, Zambesi Crescent, Maittama, Abuja, Nigeria
* Correspondence: nazerois@yahoo.fr Tel.: +237670147046

Abstract: Hybrid renewable energy systems (HRESs) are an effective tool for addressing the challenges of rural electrification in sub-Saharan Africa (SSA). However, their viability is limited by the lifespan, environmental impacts, high costs, and inefficiency of conventional energy storage technologies (battery and pumped-hydro). This study examines a hydrogen-based energy storage system, combined with photovoltaic (PV) and wind energy, for the electrification of Dargalla, a village in northern Cameroon. The goal is to meet community and agricultural electricity needs while optimising the system. The analysis utilised HOMER software to simulate, model, and optimise the system. The optimal architecture included a 50-kW PV array, a 10-kW wind turbine, a 1-kW fuel cell, a 30-kW electrolyser, a 25-kg hydrogen tank, and a 10-kW converter. The optimised system's net present cost and cost of energy were assessed at USD 138,202 and USD 0.443/kWh, respectively. Sensitivity analysis results showed that areas with high wind speeds would be mainly suitable for the proposed system. Moreover, with the upcoming decrease in the costs of fuel cells and PV components, such systems are expected to become more economically viable in the future, leading to the conclusion that integration of hydrogen-based energy storage technology in HRESs in SSA can effectively address the United Nations Sustainable Development Goals (UNSDG) and the historic Paris Climate Agreement (HCA).

Keywords: hybrid renewable energy systems; hydrogen; fuel cell; electrolizer; sub-Saharan Africa; optimization; sensitivity analysis; solar photovoltaic (PV); Wind energy.

1. Introduction

In contemporary society, electricity has emerged as an indispensable resource for ensuring a decent standard of living in both urban and rural regions [1–3]. It is crucial for the most vital tasks in our daily lives, including entertainment, transportation, education, and healthcare [4–7]. In 2019, the International Energy Agency (IEA) reported that 760 million individuals, accounting for 10% of the global population, had no electricity access [8]. Figure 1 depicts the global distribution of those lacking access to electricity. They are mainly concentrated in developing nations, particularly in sub-Saharan Africa and South Asia [9].

Most of these nations exhibit a disparity in the pace of electricity between rural and urban regions [10–12]. In this instance, Cameroon, a sub-Saharan country in Central Africa, achieved a nationwide electricity access rate of 65% in 2021, with a notable disparity between urban regions, where the rate was 95%, and rural areas, where it was only 25% [13,14]. The challenges of rural

Preprints.org (www.preprints.org) | NOT PEER-REVIEWED | Posted: 25 December 2024 doi:10.20944/preprints202412.2206.v1

electrification in sub-Saharan Africa often stem from economic, geographical, and social factors. Significant obstacles include low population density, extensive and rugged terrain, and insufficient financial resources [15].

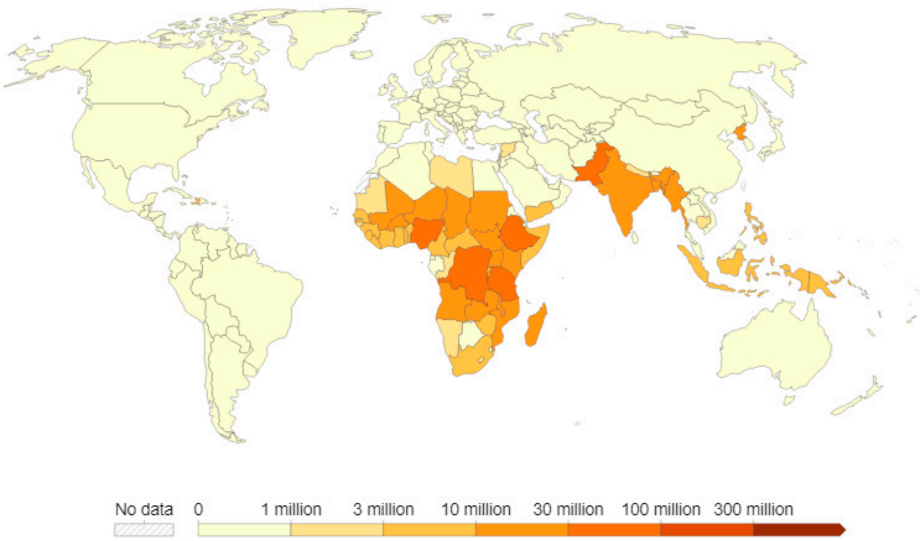

Figure 1. Global population without access to electricity by country in 2019 [9].

As a result, most individuals living in rural regions depend on alternate sources, primarily diesel generators, to meet their electrical needs. This approach is characterized by the drawbacks of noise pollution, greenhouse gas emissions, and the need for regular maintenance, which comes with a significant fuel expense.

Recently, hybrid renewable energy systems (HRESs) have been touted as an efficient way to generate electricity in rural areas of sub-Saharan Africa. An HRES consists of many power plants that utilize diverse fuels, including fossil fuels and renewable sources. Compared to single-source renewable energy systems, HRESs are characterized by higher reliability, greater efficiency, and the ability to generate power at lower costs [16–18]. There are several forms of energy storage in HRESs, with the two most frequently employed being batteries [19–28] and pumped-hydro storage (PHS) [29–39]. Nevertheless, the utilization of batteries is restricted because of environmental apprehensions and their limited duration of usage [40]. PHS, however, may significantly affect the terrain and hydrology and must be situated in places with substantial variations in elevation [41]. Hence, the objective of adopting an alternative energy storage system that overcomes the limitations of conventional energy storage devices is becoming a vital pursuit for improving the viability of HRESs in SSA.

On the other hand, hydrogen has a greater energy density than batteries, indicating its ability to store more energy per unit of weight [42–44]. It may be produced from several sources, including renewable energy sources, which makes it a potentially more sustainable choice for storing energy [45]. Hydrogen storage is adaptable to different requirements, allowing for both expansion and reduction in size to cater to a wide range of applications, spanning from individual household setups to extensive grid storage facilities. Hydrogen energy storage uses electrolysis. An electric current splits water (H2O) into hydrogen (H) and oxygen (O) gases during electrolysis ($2H_2O \rightarrow 2H_2 + O_2$) [46]. Hydrogen gas may be stored in tanks or subterranean caves for later use. Gas turbines or fuel cells may turn stored hydrogen into power when needed. Florian Klumpp [47] highlighted that by 2030, hydrogen storage will clearly be the most favorable technology for all storage-discharge routes. The features described above are the main reasons for the continued popularity of integrating hydrogen-based energy storage in HRESs.

The hydrogen-based hybrid renewable energy systems (HRESs) literature primarily focusses on optimal design-related research. These studies aim to establish the optimal number or size of system

Preprints.org (www.preprints.org) | NOT PEER-REVIEWED | Posted: 25 December 2024 doi:10.20944/preprints202412.2206.v1

components that satisfy all constraints and either minimize or maximize the objective function(s). Conducting an exhaustive review of all research undertaken on this topic is beyond the scope of this article. For example, we will highlight a few studies, including the study by Zhang et al. [48], which focused on the optimal sizing of a standalone solar/wind/hydrogen hybrid energy system in Khorasan, Iran. The study employed a hybrid search optimization technique to minimize the total life cycle cost of the HRES while considering the system's reliability. The findings demonstrated that the suggested technique outperformed previous methods in terms of performance. Using the GRHYSO software, Rodolfo et al. [49] designed and conducted a techno-economic study of grid-connected hybrid photovoltaic/wind systems for intermittent hydrogen generation. They considered the net present value (NPV) of the system as an evaluation criterion and established that in locations with high wind speed, the selling price of hydrogen should be about 10 €/kg to make economically feasible systems. Pablo et al. [50] applied a fuzzy logic-based energy management system (EMS) to optimize a standalone hybrid system that combines solar, wind, hydrogen, and battery technologies. The study spanned 25 years and demonstrated that the proposed control system successfully achieved the objectives set for the HRES's EMS. Furthermore, it resulted in a significant 13% cost reduction compared to other less advanced EMS systems based on control states. Akyuz et al. [51] studied a hybrid wind (10 kW)-photovoltaic (1 kWc) system designed for a partridge farm with an average energy consumption of 20.33 kWh/day. The study evaluated performance, energy efficiency, and hydrogen production from excess energy. The results showed a state of charge ranging from 56.6% to 88.3% from April to July, with hydrogen production of 14.4 kg in July. The electrolyzer efficiency varied from 64% to 70%, the wind-electrolyzer system efficiency from 5% to 14%, and the photovoltaic-electrolyzer system efficiency from 7.9% to 8.5%.

Torreglosa et al. [52] introduced an innovative approach for energy dispatching in off-grid photovoltaic/wind turbine/hydrogen/battery hybrid systems in Algeciras, Spain. The technique was based on Model Predictive Control (MPC), and MATLAB-Simulink was used to model the HRESs, including information from datasheets of commercially available components. Alonso et al. [53] employed the HOMER (Hybrid Optimization Model for Electric Renewable) software to assess three energy storage technology setups: the battery energy storage system (BESS), the hydrogen energy storage system (H2ESS), and the hybrid energy storage system (HESS) in both grid-connected and off-grid scenarios. The findings indicated that BESS had the highest competitiveness among the three alternative storage methods when the electric grid was accessible. According to the study, hydrogen has a complementary function when used in conjunction with batteries, enhancing the flexibility of microgrids and facilitating more extensive decarbonization. Turkdogan et al. [54] applied the HOMER software to model, simulate, and optimize an HRES consisting of solar, wind, hydrogen, and battery components. This HRES was designed to fulfil a single-family household's energy requirements, including utility and transportation loads. The results indicated that the most efficient system could produce energy and hydrogen at $0.685 per kilowatt-hour and $6.85 per kilogram, respectively. The study by Basu et al. [55] broadly examined the intermittent characteristics of renewable energy sources through hydrogen energy storage. Three energy system combinations were investigated: a hybrid system that combines solar and hydrogen, a system that combines wind and hydrogen, and a system that combines solar, wind, and hydrogen. The hybrid system was determined to have the most cost-effective levelized cost of energy (LCOE) at $0.3387 per kilowatt-hour (kWh).

The research conducted by Ramin et al. [56] applied a computer program to model and optimize HRESs that integrate wind turbines (WT), photovoltaic systems (PV), and fuel cells (FC) in four distinct sites in Iran. The study revealed that hydrogen-based hybrid renewable energy systems (HRESs) are more economically viable for off-grid applications in most locations nationwide. Jahangir et al. [57] employed the HOMER software to conduct an economic assessment of substituting conventional diesel-only backup systems with a hydrogen-only system and a hybrid hydrogen and diesel backup system in hybrid photovoltaic/wind systems. The findings indicated that the integrated diesel/hydrogen backup system has advantages in terms of cost-effectiveness and

Preprints.org (www.preprints.org) | NOT PEER-REVIEWED | Posted: 25 December 2024 doi:10.20944/preprints202412.2206.v1

environmental impact. Rodolfo et al. [58] deployed a multi-objective evolutionary algorithm (MOEA) and a genetic algorithm (GA) to achieve the optimal design of a hybrid renewable energy system (HRES) that incorporates solar, wind, diesel, hydrogen, and battery components. The objective was to minimize the total cost, pollutant emissions (CO_2) (specifically CO_2), and unmet load. The researchers concluded that the multi-objective design technique was superior to mono-objective approaches because it enables the designer to choose the optimal solution based on cost, reliability, and pollution emissions. Askarzadeh et al. [59] adopted the multi-objective Crow search algorithm (MOCSA) to optimise a grid-connected photovoltaic/diesel/fuel-cell hybrid energy system. The optimization process focused on three primary objectives: levelized cost of energy (LCOE), loss of power supply probability (LPSP), and renewability. The analysis determined that the hybrid system could sell and purchase energy from the grid. Caliskan et al. [60] conducted a study using the HOMER software to simulate and optimize a hybrid system (solar and wind energy) to evaluate its technical and economic viability in Elazig, Turkey. The study's conclusions revealed that a system combining wind and solar energy connected to the grid was economically viable and capable of meeting electricity and hydrogen needs. The system could produce 2,156,664 kWh of electricity yearly at a cost energy cost at $0.0232/kWh and a total net present cost of $7,668,500.

Table 1 provides a summary of all the research described above. This summary highlights that most research has been conducted in developed countries and rarely in developing nations, particularly in sub-Saharan Africa. Despite the high cost of hydrogen energy storage, significant cost reductions are expected, which bodes well for the future of this technology in sub-Saharan Africa.

Table 1. Selected previous hydrogen-based HRES related studies.

S No	Authors/Ref	Country Technique/software	Energy Sources	Storage Device
01	Zhang et al. [48]	Iran ANN algorithm	SPV-WES	Hydrogen
02	Rodolfo et al. [49]	Spain GRHYSO	SPV-WES	Hydrogen
03	Pablo et al. [50]	Spain MATLAB	SPV-WES	Battery – Hydrogen
04	Akyuz et al. [51]	Turkey MATLAB	SPV-WES	Hydrogen
05	Torreglosa et al. [52]	Iran MATLAB	SPV-WES	Hydrogen
06	Alonso et al. [53]	Belgium HOMER	SPV-WES	Battery – Hydrogen
07	Turkdogan et al. [54]	Turkey HOMER	SPV-WES	Battery – Hydrogen
08	Basu et al. [55]	India HOMER	SPV-WES	Hydrogen
09	Ramin et al. [56]	Iran MATLAB	SPV-WES	Battery – Hydrogen
10	Jahangir et al. [57]	Iran HOMER	SPV-WES-DG	Hydrogen
11	Rodolfo et al. [58]	Spain C++	SPV-WES-DG	Battery – Hydrogen
12	Askarzadeh et al. [59]	Iran MATLAB	SPV-DG	Hydrogen
13	Caliskan et al. [60]	Turkey HOMER	SPV-WES	Hydrogen

Preprints.org (www.preprints.org) | NOT PEER-REVIEWED | Posted: 25 December 2024 doi:10.20944/preprints202412.2206.v1

Note: ANN: Artificial Neural Network; DG: Diesel Generator; SPV: Solar Photovoltaic; WES: Wind Energy System.

Furthermore, none of these studies considered load demand in the agriculture sector. Most agricultural operations in sub-Saharan Africa occur in rural areas, where they serve as the primary means of sustenance, employing over 50% of the working population [61]. On the other hand, these studies did not consider the seasonal variation in electricity demand. Most countries in the SSA experience two types of seasons: the rainy season and the dry season. Finally, most past research that performed sensitivity analysis failed to provide practical interpretations of their findings. These interpretations are essential for comprehending various aspects of hydrogen-based HRESs and guaranteeing their sustainable development to face rural electrification challenges in SSA.

This research aims to fill the gaps found in the existing literature by applying HOMER software to optimize a photovoltaic/wind/hydrogen HRES to fulfil the power requirements of households, communities, companies, and agricultural operations in the remote area of Dargalla in the Far North region of Cameroon.

The rest of this paper is organized as follows: Section 2 describes the materials and methods used to carry out the study. Section 3 presents the acquired results, followed by Section 4, which contains the discussion part. Section 5 provides the paper's conclusion.

2. Materials and Methods

2.1. Research Methodology and Tools

The literature has identified two primary methods for analyzing and optimizing hybrid renewable energy systems (HRES): optimization techniques and software tools. A thorough examination of all these strategies is provided in [62–64]. Software tools such as HOMER, HIBRID2, and HOGA have gained significant attention in the literature for their remarkable enhancements. HOMER, initially created in 1992 by the National Renewable Energy Laboratory (NREL) in the United States, is widely acknowledged as the most often utilized and reliable tool [65–67]. HOMER is available in two versions: HOMER Legacy, which is free, and HOMER Pro, which is the commercial version [67]. The selection of HOMER Pro was justified due to its various features. The analyses were conducted on a computer with a Windows 10 Pro 64-bit operating system. The machine has an Intel(R) Core (TM) i7-4700MQ CPU running at a speed of 2.4 GHz, 8 GB of RAM, and an NVIDIA GEFORCE graphics card. HOMER is very suitable for this study since it can handle numerous energy resources and optimize their utilization effectively.

Figure 2 depicts the functional diagram of the research approach that has been executed. The HOMER program was improved by adding an initial stage that involved a thorough evaluation of the village's energy usage, available resources, and site layout. At this stage, the data obtained from surveys, expert consultations, and literature analyses were carefully reviewed to provide information consistent with HOMER and other technical and economic parameters. This methodological approach allowed for a more accurate and thorough study, making it easier to optimize the proposed HRES.

2.2. Study Location

The hybrid system to be designed is intended to meet the energy demand of the village of Dargalla, a small community within the municipality of Mora in the Far North region. It currently consists of 200 households. Table 2 provides general information about the village, and Figure 3 shows the geographical location of the study area.

2.3. Load Assessment

Energy consumption data was gathered by comprehensive surveys encompassing all population segments, including the agricultural sector, which occupies the predominant portion of the population. Table 3 comprehensively summarizes the appliances and their corresponding energy usage, and Figure 4 displays the hourly load profile during both the rainy and dry seasons.

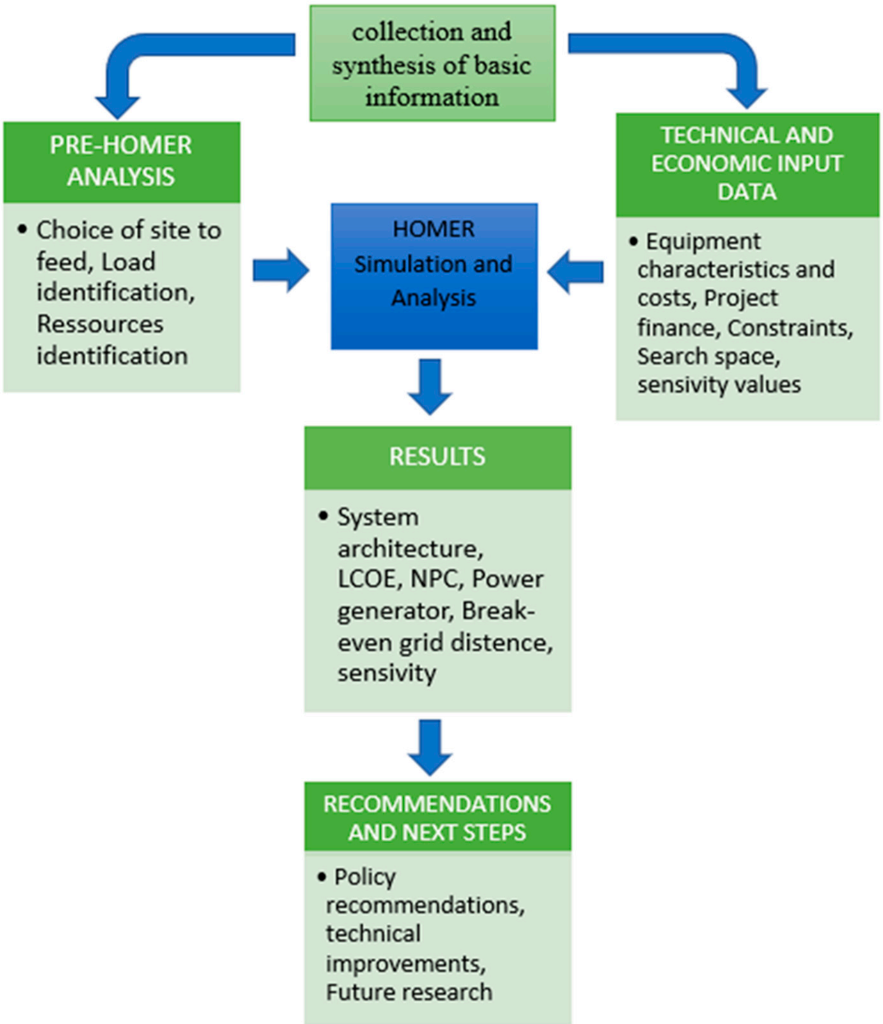

Figure 2. Functional Diagram of the Research Methodology.

Table 2. General Information about the Study Location.

Designations	Information
Country	Cameroon
Region	Far North
Division	Diamaré
Municipality	Mora
Latitude	11°2.8′N
Longitude	14°8.4′E
Elevation above sea level	75 m
Number of households	200
Nearest power transformer	8 km
Main socio-economic activities	Agriculture and livestock farming

Preprints.org (www.preprints.org) | NOT PEER-REVIEWED | Posted: 25 December 2024 doi:10.20944/preprints202412.2206.v1

Figure 3. Geographical Location of the Study Area.

Table 3. Appliances' requirement and rating for different sectors of energy consumption.

Load Type	Appliances	Rating (W)	Quantity	Total (KW)
A-Domestic				
	CFL	0.015	350	5.25
	Radio	0.012	160	1.92
	Mobile charger	0.12	160	1.92
	Fan	0.04	350	14
	TV	0.065	160	10.4
B-Community				
Health center	CFL	0.015	6	0.09
	Fan	0.04	6	0.24
	Refrigerator	0.5	2	1
	Computer	0.075	2	0.15
Street Lamp	CFL	0.1	20	2
Four mil		4.8	3	14.4
Church	CFL	0.015	4	0.06
	Fan	0.04	4	0.16
	Microphone	0.001	1	0.001
	Loudspeaker	1	3	3
C-Agricultural				
water irrigation pump		2.2	3	6.6
Electric grass-cutting machine		1.5	2	3
Trashing machine		4	2	8

Note: CFL: compact fluorescent lamp; TV: Television.

 doi:10.20944/preprints202412.2206.v1

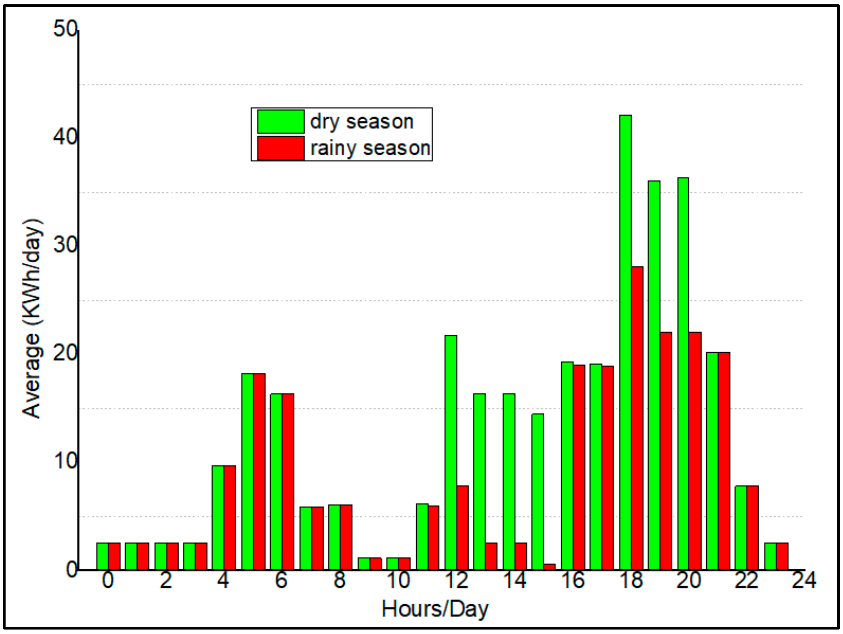

Figure 4. Average electricity demand per hour of the day, during rainy and dry seasons.

The peak power use occurs from 6 PM to 9 PM when nearly all domestic appliances are utilized. This finding aligns with research conducted by [68,69], indicating that energy consumption reaches its highest point during the nighttime hours in Africa. The energy usage in Dargalla daily is 96.21 KWh/day in the rainy season and 190.47 KWh/day in the dry season. The research conducted with the HOMER Pro program included hourly fluctuations of 20% and daily fluctuations of 10%.

2.4. System Configuration

Figure 5 depicts the diagram of the proposed Hybrid Renewable Energy System (HRES). The system comprises various components, including a photovoltaic generator, wind turbines, an electrolyzer, a fuel cell system, a converter, and a hydrogen storage tank. When the combined energy output of the photovoltaic panels and wind turbines exceeds demand, the electrolyser uses the surplus to produce hydrogen gas. This gas is then stored in the hydrogen tank (HT). The fuel cell system then converts the stored hydrogen gas back into electricity when the combined production of the photovoltaic panels and wind turbines is less than demand. The proposed HRES, modelled by HOMER software, is presented in Figure 6.

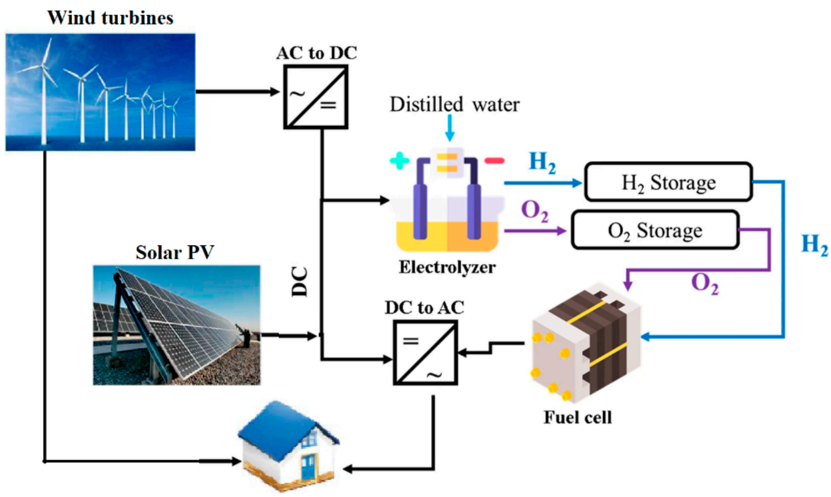

Figure 5. The schematic diagram of the proposed HRES.

Preprints.org (www.preprints.org) | NOT PEER-REVIEWED | Posted: 25 December 2024 doi:10.20944/preprints202412.2206.v1

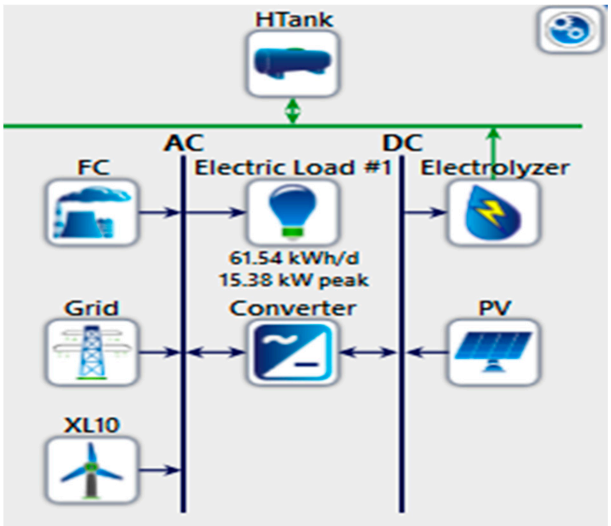

Figure 6. The proposed HRES in HOMER software.

2.5. Assessment of Available Solar and Wind Resources

The data on solar radiation and wind speed at the study's location, Dargalla, was collected from the NASA Surface Meteorology and Solar Energy (SSE) database [70]. The coordinates used for this data collection were those of Mora (11°2.8'N, 14°8.4'E), the nearest point of data available. Wind velocity measurements were gathered for 29 years, from January 1984 to December 2013. The site documented a yearly mean wind velocity of 5.15 m/s at 10 meters above the ground. Figure 7 presents the data on the average wind speed for each month.

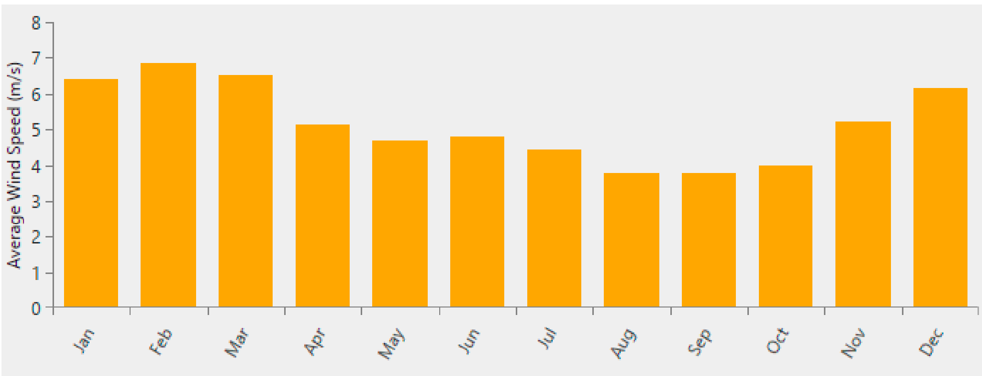

Figure 7. Monthly Average Wind Speed Measured at 10 m at the Study Site.

Figure 8 illustrates the mean daily monthly solar radiation and clearness index for a 22-year period from July 1983 to June 2005. These data were used as input for the hybrid system model. This graph illustrates the region's remarkable capacity to harness solar energy using photovoltaic panels. The annual average solar radiation is 5.82 kWh/m²/day, with an average clearness index of 0.54. Regarding solar radiation, March experienced the most significant amount with 6.670 kWh/m²/day, whereas August had the lowest value at 4.98 kWh/m²/day.

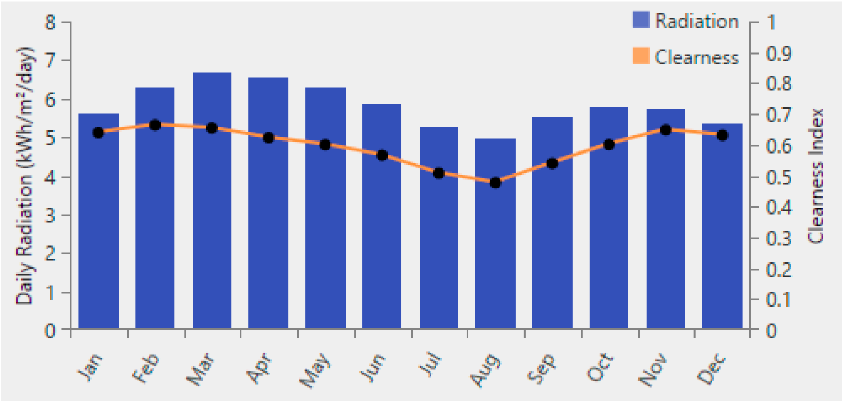

Figure 8. Monthly Average Solar Resources at the Study Site.

2.6. System Analysis

2.6.1. Photovoltaic Array

The PV solar module used in this research was the SPR-E20-327, a monocrystalline module produced by Sunpower. The module has a power rating of 327 watts peak (Wp) and can generate a maximum direct current (DC) voltage of 600 volts (V). Table 4 displays the precise technical details of the selected PV module. HOMER implements the equation provided in reference [71] to compute the output of a photovoltaic (PV) array:

$$P_{output} = Y_{PV} f_{PV} \left(\frac{G_T}{G_{T,STC}}\right) \left[1 + \alpha_P \left(T_c - T_{c,STC}\right)\right], \quad (1)$$

where f_{PV} represents the PV derating factor in percentage (%), Y_{PV} is the rated capacity of the PV array in kilowatts (kW), G_T the global solar radiation incident on the surface of the PV array, measured in kilowatts per square metre (kW/m²). $G_{T,STC}$ represents the standard amount of incident radiation at the standard test condition, which is 1 kW/m² at a temperature of 25°C. α_P represents the temperature coefficient of power, expressed as a percentage per degree Celsius (%/°C). T_c and $T_{c,STC}$ are the PV cell temperature in degrees Celcius (°C) at the actual and under the standard test conditions, respectively. HOMER applies the Graham and Hollands approach to calculate the hourly global solar radiation based on the monthly average global solar radiation [71]. The temperature coefficient of power for the selected module is -0.38%/°C as indicated in Table 6 of the technical specifications of the said PV module. The derating factor considered in this study was 0.95. The PV system was expected to have a lifespan of 25 years and a total capital cost, replacement cost, and operation and maintenance cost of 3000 €/kW, 3000 €/kW, and 10 €/kW/year, respectively [72].

Table 4. PV module specifications [73].

Item	Specification
Manufacturer	Sunpower
PV Module type	Mono-si
Module number	SPR-E20-327-C-AC
Module efficiency	20.4 %
Power capacity	327 W
Power tolerance	+5/-0%
Rated voltage (Vmpp)	54.7 V
Rated current (Impp)	5.98 A
Open-Circuit Voltage (VoC)	64.9 V
Short-Circuit Current (ISC)	6.46 A
Maximum system voltage	DC 600 V

Power Temp Coef	-0.38%/°C
Volt Tem coef	-175mV/°C
Current Temp Coef	3.5mA/°C
Dimensions	46mm×1,559mm×1,046mm
Operating temperature	-40 º C - +85º C
area	1.63 m²
Weight	18.60 kg

2.6.2. Wind Turbine

The wind turbine (WT) model considered in this study is the bergey excel 10-R model, manufactured by Bergey Windpower. The nominal power of of the system is 10 kW at a wind speed of 12 m/s. The turbine's technical characteristics are detailed in Table 5, and its power curve is displayed in Figure 9. The power law was used to calculate wind speed at the hub height [65]:

$$V_{hub} = V_{anem} \cdot \left(\frac{Z_{hub}}{Z_{anem}}\right)^{\alpha}, \quad (2)$$

where, V_{hub} and V_{anem} represent the wind speeds at the hub and anemometer height (Z_{hub}, and Z_{anem}). The power law exponent α, which typically has a value of 0.14 for low roughness sites, is also included in the equation [65]. HOMER software also uses Equation (3) to find the wind turbine output power $P_{WT}(t)$ at any time t [74].

$$P_{WT}(t) = \begin{cases} aV^3(t) - bP_R & V_{Ci} < V(t) < V_r \\ P_R & V_r < V(t) < V_{Co} \\ 0 & \text{Otherwise} \end{cases}, \quad (3)$$

where V_r, represents the rated speed, V_{Ci} is the cut-in speed, V_{Co} is the cut-off speed, and P_R represents the wind turbine's rated power. a and b are defined by equations (4) and (5):

$$a = \frac{P_R}{V_r^3 - V_{Ci}^3}, \quad (4)$$

$$b = \frac{V_{Ci}^3}{V_r^3 - V_{Ci}^3}, \quad (5)$$

The total initial cost, replacement cost, and operation and maintenance cost were estimated at 50,000 €/unit, 30,000 €/unit, and 200 €/year [75]. The turbine's estimated lifespan was 20 years.

Table 5. Technical specifications of the selected wind turbine model [76].

Item	Specification
Manufacturer	Bergey WindPower
Model	Bergey excel 10-R
Nominal power	10 kW at 12 m/s
Cut-in Wind Speed	2.5 m/s
Cut-Out Wind Speed	None
Furling Wind Speed	14-20 m/s
Max. Design Wind Speed	60 m/s
Temperature range	-40 to +60 °C
Hub height	30 m
Type	3 Blade Upwind

Preprints.org (www.preprints.org) | NOT PEER-REVIEWED | Posted: 25 December 2024 doi:10.20944/preprints202412.2206.v1

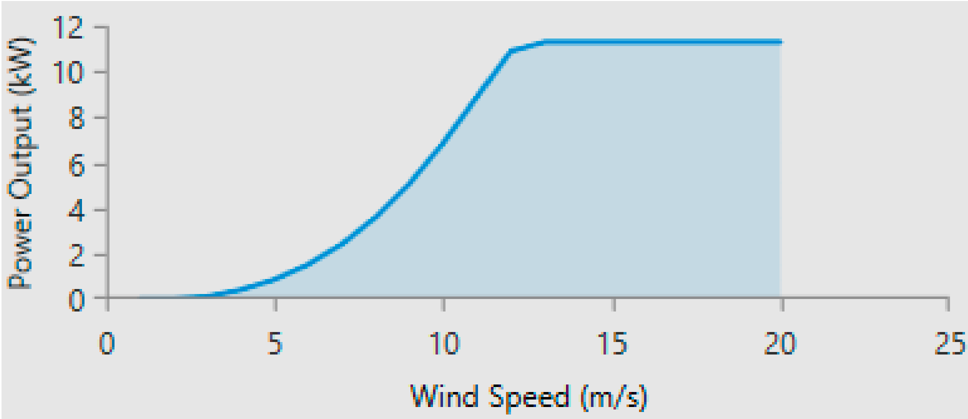

Figure 9. The power curve of the selected wind turbine.

2.6.3. Fuel Cell

The Fuel Cell (FC) is an electrochemical system that produces electrical energy by converting chemical energy from hydrogen fuel and oxygen. The FC is believed to be a more energy-efficient technology than traditional energy sources since it directly transforms hydrogen fuel into electrical energy without any intermediate combustion stage [77]. In this study, the proton exchange membrane fuel cell (PEMFC) was adopted because of its electrical efficiency, reduced weight, extended cell lifespan, compact size, ability to operate at various temperatures, rapid start-up times, absence of pollutants, cost-effectiveness, minimal maintenance requirements, silent operation, and high adaptability [78].

The output voltage E_{cell} of a fuel cell stack is given by equation (6) [65]:

$$V_{FC} = N_{cell}E_{cell} = E - V_{act} - V_{ohm} - V_{con} \tag{6}$$

where V_{FC}, E, $Vact$, V_{ohm} , and V_{con} are the output voltage, open-circuit voltage, activation overvoltage, ohmic overvoltage, and concentration overvoltage, respectively.

2.6.3. The Electrolyzer

Industries use large-scale hydrogen generation from water electrolysis using renewable energy sources [79]. Water electrolysis splits molecules into hydrogen and oxygen using electricity. Marketed electrolyzers include polymer electrolyte membrane (PEM), phosphoric acid, solid oxide, direct methanol, and alkaline [80]. The PEM electrolyser (EL) is best for small energy systems in remote rural areas. The PEM electrolyzer's theoretical efficiency is 94% due to its excellent heating value. In practice, this figure is 85% [81]. Hydrogen production rate by is computed by (7) [74].

$$Q_{H2} = \eta_f \frac{N_{cell}I_{cell}}{2F} \tag{7}$$

where η_f is the Faraday efficiency, $Ncell$ is the number of cells connected in series, I_{cell} is the current in the electrolyzer, and F is the Faraday constant.

2.6.3. The Hydrogen Tank

The hydrogen generated by the electrolyzer is pressurized using a compressor and stored in a tank. The power required for compression (P_{comp}) is indicated as [74] :

$$P_{comp} = \frac{\gamma}{\gamma - 1} R \frac{T}{\eta_C} \left[\left(\frac{P_2}{P_1}\right)^{\frac{\gamma-1}{\gamma}} - 1 \right] Q_{H2} \tag{8}$$

The equation's parameters are as follows: γ represents the polytrophic coefficient, R represents the gas constant, T represents the compressor inlet temperature, η_C represents the compressor

Preprints.org (www.preprints.org) | NOT PEER-REVIEWED | Posted: 25 December 2024 doi:10.20944/preprints202412.2206.v1

efficiency, P_1 and P_2 represent the inlet and outlet pressure, respectively, and Q_{H2} represents the mass flow rate of hydrogen.

The pressure of hydrogen in the tank, denoted as P_{tank}, is determined by the following equation [82]:

$$P_{tank} = \frac{RT}{V_{tank}} n_{tank} \tag{9}$$

where V_{tank} and n_{tank} are the volume of the tank and the number of moles of gas in the tank, respectively.

2.6.3. The Converter

Power transfer between the DC and AC buses is facilitated by a converter (CON) that converts direct current (DC) to alternating current (AC) by an inverter, or vice versa, from AC to DC through a rectifier, depending on the electrical load. This guarantees the effective fulfilment of energy requirements while preserving an ideal energy transfer between the two buses. This study utilised a generic system converter with a lifespan of 25 years, an efficiency of 95%, a capital cost of $40/kW, and yearly operation and maintenance costs of $10/kW/year [72].

2.7. Simulation, Optimisation and Sensitivity Analysis

2.7.1. The Evaluation Criteria

HOMER uses the net present cost (NPC) and the levelized cost of energy (LCOE) as the evaluation criteria for determining the best system design. Based on the NPC, all possible system configurations in the optimization results are ranked. The NPC represents the aggregate of all the present values of expenses and incomes linked to the system, taking into account the discount factor. These two assessment criteria are detailed as:

$$\begin{cases} NPC = \dfrac{C_{ann,tot}}{CRF(d,N)} \\ C_{ann,tot} = C_{ann,cap} + C_{ann,rep} + C_{ann,O\&M} + C_{ann,fuel} - R_{ann,salv} \\ CRF = \dfrac{i(1+d)^N}{(1+d)^N - 1} \\ d = \dfrac{i-f}{1+f} \\ LCOE = \dfrac{C_{ann,tot} - C_{boiler} \cdot H_{thermal}}{E_{served}} \end{cases} \tag{10}$$

The parameters $C_{ann,tot}$, $C_{ann,cap}$, $C_{ann,rep}$, $C_{ann,O\&M}$, $C_{ann,fuel}$, $R_{ann,salv}$, CRF represent the total annualized cost of the system ($/year), annualized capital ($/year), replacement ($/year), maintenance costs of all system components ($/year), annualized cost of fuels used to feed the power generators ($/year), annualized total savage value of all system components ($/year), and capital recovery factor. *CFR* depends on the discount rate (*d*) and project lifespan (*N*). The discount rate is, in turn, expressed as a function of the annual inflation rate (*f*) and nominal interest rate (*i*). $H_{thermal}$, E_{served}, *COE*, and C_{boiler} represent the total thermal load served (kWh/year), total electric load served (kWh/year), levelized cost of energy ($/kWh) and the boiler marginal cost ($/kWh). Given that the system is not serving any thermal load, $H_{thermal} = 0$. This article considered nominal interest and inflation rates of 8% and 3%, respectively [83].

2.7.2. Dispatch Strategies

A dispatch strategy refers to rules that dictate how the generator(s) and storage device(s) operate. HOMER software can simulate two dispatch strategies: load following (LF) and cycle charging (CC) [84]. In the load-following strategy, a generator only produces the necessary power to meet the demand. On the other hand, in the cycle charging strategy, a generator operates at full

Preprints.org (www.preprints.org) | NOT PEER-REVIEWED | Posted: 25 December 2024 doi:10.20944/preprints202412.2206.v1

capacity each time it is turned on, with any excess power being stored in the power storage device. Both the load following and cycle charging strategies were considered in this study.

2.7.3. Optimization Variables and Search Space

An optimization variable, also known as a decision variable, is one the system designer may adjust. During the optimization process, HOMER explores multiple possible values of this variable. Table 6 presents the optimization variables used throughout this investigation and their associated values.

Table 6. Optimization variables of the study model.

Optimization variable	PV array size (kW)	Number of WT	hydrogen tank capacity (Kg)	Fuel Cell Capacity (KW)	Electrolyzer capacity (KW)	Converter capacity (kW)
Maximum	150	7	250	25	160	25
Minimum	0	0	0	0	0	0
Step	25	1	25	5	20	5
Number of values	7	8	11	6	9	5

The variables considered in the optimization process where the size of the photovoltaic generator (seven values), the number of wind turbines (eight values), the capacity of the hydrogen tank (eleven values), the size of the fuel cell generator (six values), the size of the electrolyzer (nine values), and the size of the bidirectional converter (five values). The search space encompasses the range of potential system configurations HOMER examines to identify the most effective solution. This study conducted simulations for each possible combination of the six optimization variables for distribution strategies: LF and CC. Therefore, the HOMER software simulated a total of 332640 (7×8×11×6×9×5×2) combinations.

2.7.4. Constraints

System configurations must meet constraints. A non-conforming design is unfeasible and is not evaluated by HOMER during simulation and optimization. In this case study, two constraints are considered:

- The Maximum annual capacity shortage constraint is related to the maximum yearly capacity deficiency, set at 5% in this study. HOMER eliminated systems that did not meet at least 95% of the annual electrical and operating reserve.
- Operating reserve constraints impose surplus operational capacity to maintain system resilience in the case of a sudden demand increase or reduction in renewable energy output. HOMER uses four inputs to determine the required operating reserve: two of which are expressed as a percentage of the variability of the electricity demand (current time step and annual peak load), and two of which are expressed as a percentage of renewable energy production (wind power output and solar power output). In this case study, the operating reserve percentages associated with the load in the current time step, annual peak load, solar power output, and wind power wind output were established at 10%, 0%, 80%, and 50%.

Feasible configurations are those that satisfy all of the aforementioned constraints. Those not meeting at least one of these constraints are considered unfeasible.

2.8. Sensitivity Analysis

Sensitivity analysis evaluates how input data variations influence a model's output data. Within the context of HRES optimization, this analysis investigates the influence of changes in meteorological (wind speed, solar radiation, etc.), economic (capital cost of components, O&M cost

Preprints.org (www.preprints.org) | NOT PEER-REVIEWED | Posted: 25 December 2024 doi:10.20944/preprints202412.2206.v1

of components, fuel cost, inflation rate, interest rate, etc.), and technical (maximum capacity shortage, etc.) parameters on the optimal HRES. The term "sensitivity variable" sometimes refers to a parameter involved in a sensitivity analysis. The designer inputs a range of values, or sensitivity values, into HOMER for each sensitivity variable. This study investigated the following sensitivity variables: wind speed, solar radiation, the initial and replacement cost of the fuel cell, the initial and replacement cost of photovoltaic (PV) panels, and capacity shortage. Table 7 lists these sensitivity variables and their respective value ranges.

Table 7. Sensitivity variables and associated values.

Sensitivity variable	values
Wind speed (m/s)	4,5,5.8, 7, 8
Solar radiation (kWh/m²/d)	4,5.1,6, 7, 8
Capital and replacement cost multiplier of PV	0.25, 0.5, 0.75, 1
Capital and replacement cost multiplier of Fuel Cell	0.25, 0.5, 0.75, 1
Maximum capacity shortage (%)	0, 2.5, 5, 7.5, 10

The sensitivity analyses were executed sequentially to expedite the process, rather than simultaneously. The initial step was to conduct a sensitivity analysis of solar radiation and wind speed to account for the significant variability in the availability of these two resources and, as a result, to gain a more comprehensive understanding of the performance of hydrogen-based HRESs in the sub-Saharan region.

This was followed by a sensibility analysis of the capital costs of PV and fuel cell components, which was conducted using cost multipliers. The objectives of the study were as follows: 1) to evaluate the impact of the adoption of PV investment subsidies on the viability of hydrogen-based HRESs; 2) to understand how Hydrogen-based HRESs are promising in addressing rural electrification challenges in SSA considering the upcoming cost reductions of solar PV and fuel cell. Lastly, the sensitivity analysis of the maximum capacity shortage was carried out to better manage the trade-off between the reliability and cost of the proposed system.

2.9. The Grid Extension

The break-even grid extension distance (D_{grid}) is the distance from the grid at which the total annualized cost of the grid extension equals the total annualized cost of the proposed stand-alone system. The proposed HRES is more cost-effective than the grid extension for the electrification of the village after this point before the grid extension is more cost-effective. The break-even grid extension is determined by the following formula [75]:

$$D_{grid} = \frac{TAC - c_{power} \cdot E_{demand}}{c_{inv} \cdot CFR(i, N) + c_{om}}, \quad (11)$$

where TAC represents the total annualized cost of the stand-alone system in dollars ($), and N denotes the project's lifetime in years. E_{demand} represents the total annual power demand in kilowatt-hours per year (kWh/year), c_{power} represents the cost of grid power in dollars per kilowatt-hour ($/kWh). c_{inv} represents the investment cost of grid extension in dollars per kilometer ($/km), and c_{om} represents the operation and maintenance cost of grid extension in dollars per year per kilometer ($/yr/km).

According to [67], the estimated investment cost of the grid extension is $14,000 per kilometer and the estimated operation and maintenance cost is $300 per year per kilometer. The average price of grid electricity in Cameroon is $0.1 per kilowatt-hour [67].

3. Results

This section presents the outcomes of the analyses above. First, the optimisation results are presented, and then the results of the sensitivity analyses are described.

Preprints.org (www.preprints.org) | NOT PEER-REVIEWED | Posted: 25 December 2024 doi:10.20944/preprints202412.2206.v1

3.1. Optimization Results

The HOMER simulation and optimisation processes yielded data indicating that out of the 332,640 system configurations in the HOMER search space, only 196,790 were deemed feasible. These configurations were divided into five groups based on their system architecture: Category 1 (PV/WT/CON/FC/EL/HT), Category 2 (WT/FC/CON/EL/HT), Category 3 (PV/WT/FC/EL/HT), Category 4 (WT/FC/CON/EL/HT), and Category 5 (PV/FC/EL/HT). Table 10 presents particular information on the components, technical details, and economic parameters of the top-performing hybrid system in each category. The top-performing hybrid system in Category 1, which was the overall optimal, consisted of an 50 kW PV array, one wind turbine, a 10 kW fuel cell, a 30 kW electrolyzer, a 25 kg hydrogen tank, and a 10 kW converter with a load following dispatch strategy. The system's cost of energy (COE) and total net present cost (NPC) were $0.451/kWh and $138,202, respectively.

Table 8. Optimization results.

	Specification	**Unit**	**Best hybrid system per category**				
			Category 1	Category 2	Category 3	Category 4	Category 5
System architecture	PV array	kW	50	100	50	0	125
	Wind turbine	Number	1	0	3	5	0
	Hydrogen Tank	kg	25	25	175	200	175
	Electrolyser	KW	30	30	20	20	100
	Fuel Cell	kW	10	10	5	5	10
	Converter	KW	10	10	0	15	0
	Dispatch strategy	LF or CC	CC	CC	CC	CC	CC
Cost	LCOE	$/kWh	0.451	0.456	0.529	0.680	0.715
	NPC	$	138,202	144,342	165,916	212,690	223,902
	Total O & M cost	$/year	5,960	7,263	3,935	4,041	11,957
	Total capital cost	$	52,963	40463	109638	154,750	52,888
Power production	PV array	kWh/year	92,436	184,873	92,436	0	231,091
	Wind turbine	kWh/year	23,517	0	70,550	117,584	0
	Fuel Cell	kWh/year	7,321	12,937	6,063	4,466	21,890
	Total electricity production	kWh/year	123,274	197,810	169,050	122,049	252,980
	Capacity shortage	kWh/year (%)	1,044 (4.65)	558 (2.49)	1,144 (5.1)	1,119 (4.98)	788(3.51)
	Unmet load	kWh/year (%)	641 (2.86)	334(1.49)	539(2.4)	601 (2.68)	572 (2.55)
	Excess electricity	kWh/year (%)	24,254 (14.7)	41,182 (20.8)	83,149 (49.2)	47,813(39.2)	4,263 (1.69)
Capacity factor	PV array	%	21.1	21.1	21.1	0	21.1

Preprints.org (www.preprints.org) | NOT PEER-REVIEWED | Posted: 25 December 2024 doi:10.20944/preprints202412.2206.v1

Wind turbine	%	26.8	0	26.8	26.8	0
Fuel Cell	%	8.36	14.8	13.8	10.2	25

The analysis of the optimal system's NPC, as shown in Figure 10, reveals that about 50% of its variation was attributed to the overall operation and maintenance (O&M) cost of the system. That high share of O&M cost in the system's NPC was due to the high O&M cost of the fuel cell component.

Figure 11 shows the electrical energy production in kW of the different power generators of the system for a typical day in mid-August (rainy season). The photovoltaic generator is active between 6 AM and 6 PM with a production peak of 38.22 kW at noon. The electrolyzer captures the energy surplus between 9 AM and 4 PM to produce hydrogen. The unmet load is very low (≈0%) between 1 AM and 4 AM but rises to 4% between 5 AM and 6 AM. The fuel cell, which consumes the stored hydrogen, starts to meet the load as soon as the photovoltaic panels cease their activity. The wind turbine generator supports this task.

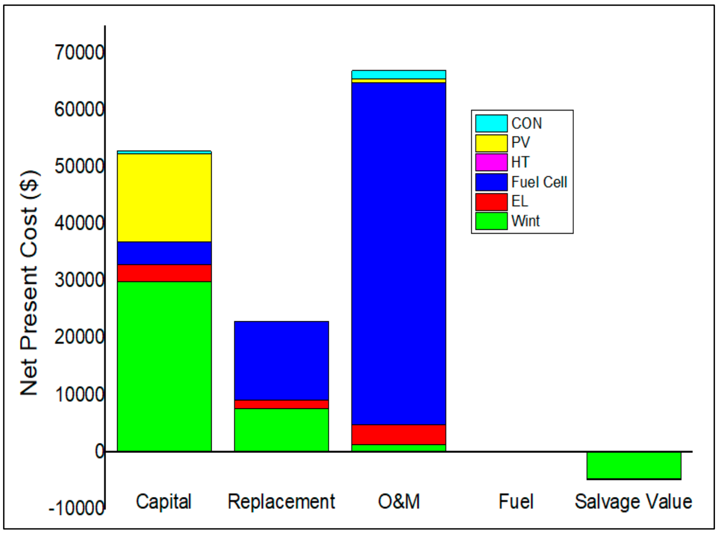

Figure 10. Cash flow summary based on the optimised architecture.

Figure 12 shows the distribution of energy production by source for each month of the year. The production peak is recorded in March. The three generators produce 123,274 kWh/year. The system's capacity shortage amounted to 641 kWh/year, equivalent to 2.86% of the demand load. This falls below the maximum allowed shortage capacity of 5%, which is a specified constraint.

Preprints.org (www.preprints.org) | NOT PEER-REVIEWED | Posted: 25 December 2024 doi:10.20944/preprints202412.2206.v1

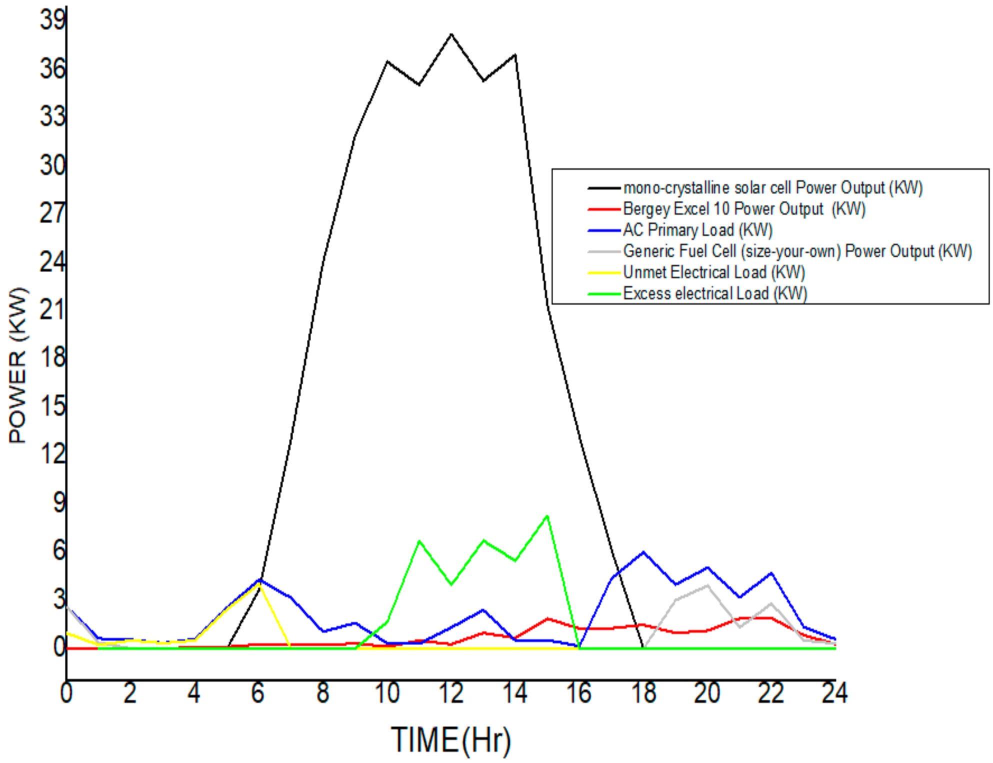

Figure 11. Operations schedules and energy flow of the system components over a 24-hour period.

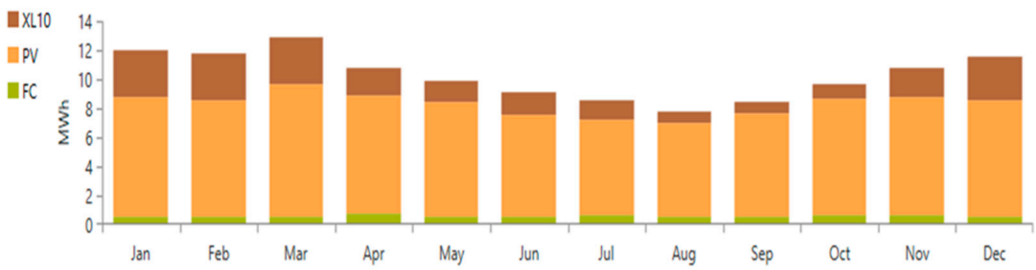

Figure 12. Monthly average electrical output from the optimal configuration system**.**

Figure 13 depicts the electrolyzer consumption, the amount of hydrogen accumulated in the tank, and the power delivered by the fuel cell over one year. The electrolyzer primarily operates during daylight hours (6 AM - 6 PM), with power peaks coinciding with periods of maximum solar energy production. Annually, it produces 1555 kg of hydrogen and consumes 76,688 kWh. The hydrogen tank, initially containing 2.5 kg at the beginning of the year, reaches a capacity of 20.5 kg at the end of the year, providing an autonomy of 325 hours. The tank level fluctuates throughout the seasons, with higher levels during the daytime and lower at night. This suggests that hydrogen production and storage primarily occur during periods of high solar energy production. The fuel cell is active between 6 PM and 6 AM, providing a stable and continuous energy source and filling the gaps when renewable sources are insufficient. It generates 7,321 kWh per year, with more pronounced electricity production between 6 PM and 11 PM. These three components work in synergy to ensure continuous and stable energy production in a hybrid system.

Preprints.org (www.preprints.org) | NOT PEER-REVIEWED | Posted: 25 December 2024 doi:10.20944/preprints202412.2206.v1

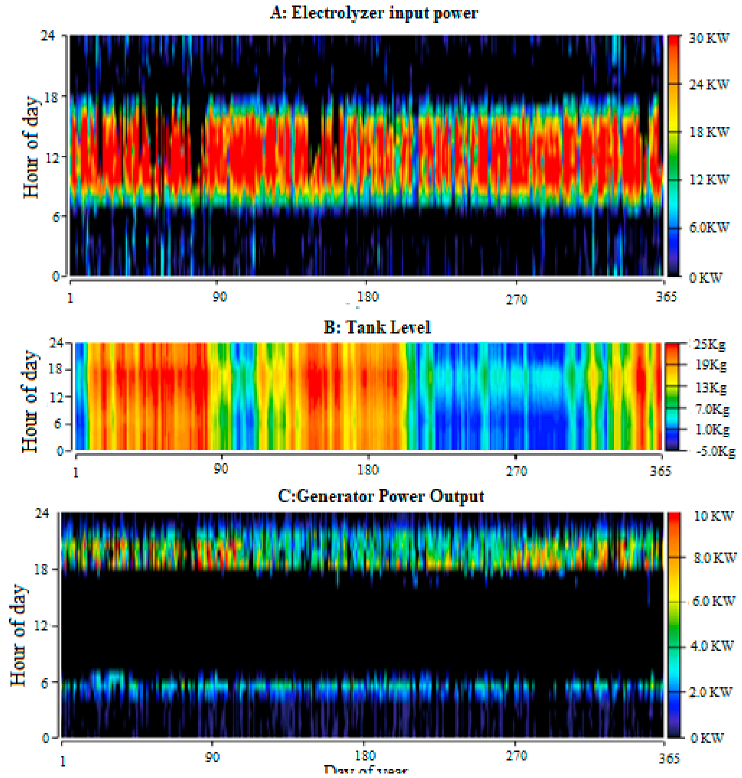

Figure 13. (A) Electrolyzer input power, (B) Tank level, (C) Full cell power output.

Figure 14 depicts the result of the comparative analysis between the Net Present Cost (NPC) of the developed standalone system and grid expansion for the electrification of Dargalla. This analysis reveals a breakeven distance for grid extension of 5.91 km, leading to the inference that the designed standalone system is a better solution than the grid extension for the electrification of Dargalla, given that the nearest power transformer is located in Mora, at a distance of 8 km.

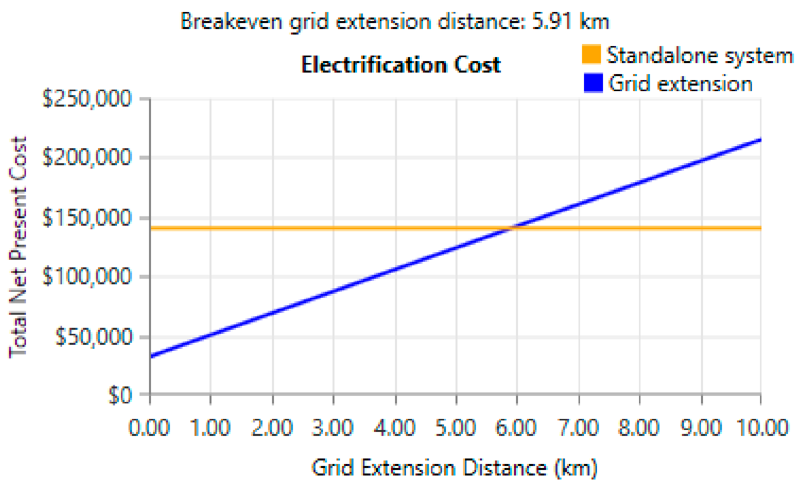

Figure 14. Cost of electrification options of Dargalla.

3.2. Sensitivity Results

Figure 15 displays the sensitivity analysis results for wind speed and solar radiation. For low wind speeds, below 4.80 m/s, the most suitable system configuration would be FC/PV/HT/EL, whatever the solar radiation. The cost of energy (COE) and net present cost (NPC) of the system would not be affected by changes in wind speed, as there would be no wind turbine included in the system.

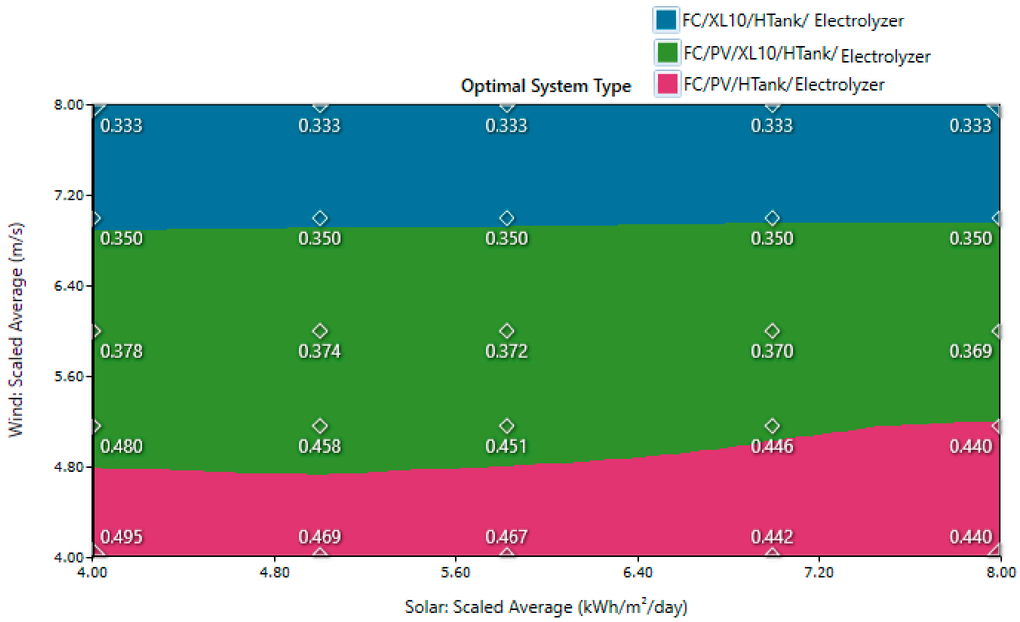

Figure 15. Results of the Sensitivity Analysis of Wind Speed and Solar Radiation.

However, the wind speed will eventually approach a threshold value when the solar radiation value increases. Beyond this barrier, the best system type would be FC/PV/WT/HT/EL. By surpassing the threshold above value, the wind speed would exceed another threshold value; at this point, the most suitable system type would be FC/WT/HT/EL. The first wind speed threshold value mentioned above slightly increases as solar radiation increases. In contrast, the second threshold value is fixed at 6.80 m/s regardless of the solar radiation. The system does not include the PV array when the wind speed exceeds this value. As a result, the system's performance is not affected by changes in solar radiation. Moreover, these results clearly show that wind speed has a higher impact on the COE than solar radiation, indicating that such a system would be more viable in areas with high wind speed (Kenya, Mali, northern Nigeria [85,86]) than those with high solar radiation.

Figure 16 depicts the results of the maximum capacity shortage. enhancing the system's reliability by reducing the maximum capacity shortage from 5% to 2.5% would lead to a 0.5% increase in NPC and a 0.3% rise in COE. A reduction to 0% would result in a corresponding rise of 7% and 5%. Conversely, if the system reliability is compromised by considering a maximum yearly capacity shortage of 10%, its NPC and COE would reduce by 5% and 4%, respectively. This outcome indicates that the system has the potential to attain enhanced reliability without significantly raising the COE.

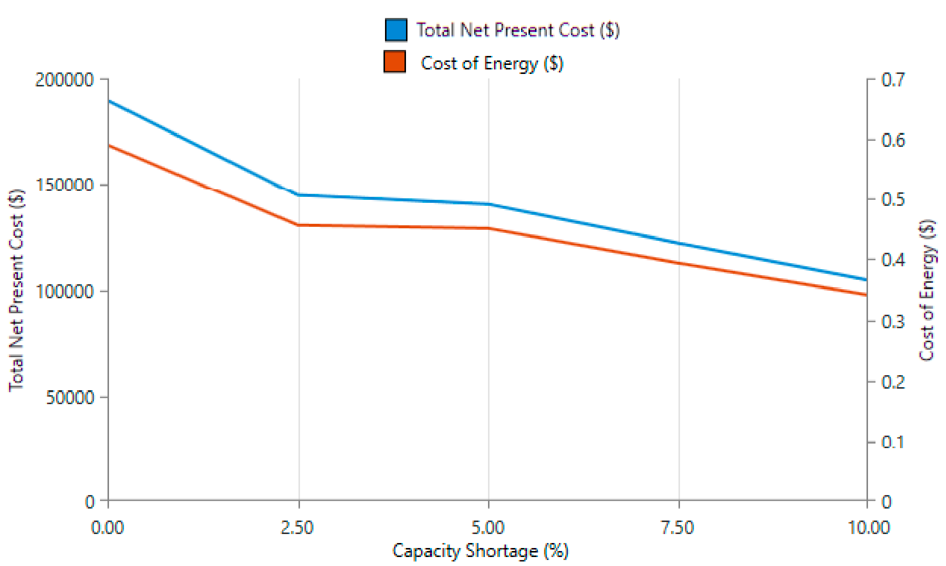

Preprints.org (www.preprints.org) | NOT PEER-REVIEWED | Posted: 25 December 2024 doi:10.20944/preprints202412.2206.v1

Figure 16. Results of the Sensitivity Analysis of Maximum Capacity Shortage.

Figure 17 illustrates the results of sensitivity analysis of capital expenditures and replacement costs of hybrid systems, highlighting the optimal configurations and their corresponding energy costs. When the acquisition and replacement costs of photovoltaic (PV) systems and fuel cells (FC) are low, the optimal configuration consists of fuel cells, photovoltaic systems, a hydrogen tank, and an electrolyzer. However, when these costs are high, the optimal configuration also includes a wind turbine. If the acquisition and replacement costs of PV systems increase from 0.5 to 1, the cost of energy increases by 10%. If these costs decrease from 1 to 0.25, the cost of energy is reduced by 24%. If the acquisition and replacement costs of FCs increase from 0.55 to 1, the cost of energy (COE) increases by 6%. If these costs decrease from 1 to 0.25, the COE is reduced by 9%. The sensitivity analysis demonstrates that fluctuations in capital expenditures and replacement costs of PV and FC systems have a significant influence on the optimal configuration of the hybrid system. Reducing these component costs favors simpler configurations (without a wind turbine), while higher costs would require the integration of additional solutions, such as wind turbines, to optimize energy costs. Over the past five years, fuel cell costs have been halved due to improvements in efficiency and durability [87].Furthermore, advancements in material selection and the enhancement of platinum-based catalyst structures have improved catalytic performance and reduced costs [88]. This has made the fuel cell a crucial element in advancing hydrogen as an energy source. Moreover, PV systems hold promise for addressing rural electrification challenges in sub-Saharan Africa. It is anticipated that the investment cost of PV systems will decrease by 50% by 2040 [89].

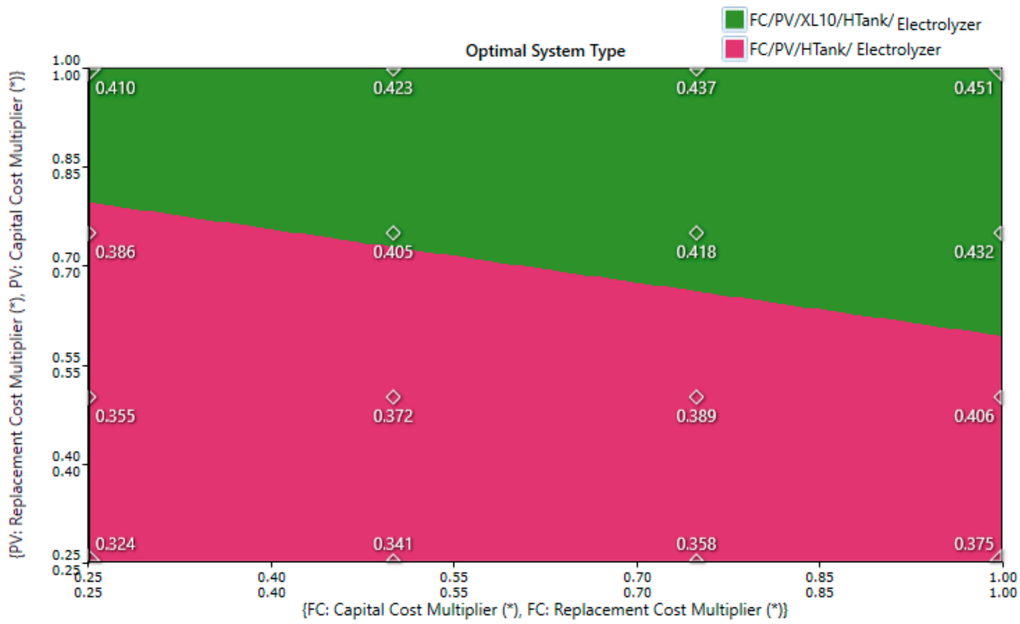

Figure 17. Results of the sensitivity analysis of the capital and replacement costs of PV and FC.

4. Discussion

The conclusions drawn from the previously presented analyses unequivocally demonstrate that the proposed system is capable of meeting the energy needs of an isolated village at a cost of energy (LCOE) lower than those that employ a storage system other than hydrogen in sub-Saharan Africa [90–95]. Each case studied uses a battery system or a pumped hydroelectric storage (PHS) system as energy storage devices, thus highlighting the technical and economic superiority of hydrogen-based hybrid renewable energy systems compared to systems relying on batteries, PHS, or diesel generators. This confirms the hypothesis stated in the introductory section. Furthermore, unlike previous studies, the system evaluation was preceded by a thorough analysis of electricity demand, encompassing all electricity-consuming sectors, including agriculture, which is the primary employment sector in rural sub-Saharan Africa. This suggests a more authentic and credible assessment of load demand, thereby contributing to the literature on the applications of hybrid renewable energy systems (HRES) in sub-Saharan Africa.

Hydrogen is a fundamental element in the transition towards cleaner energy and the reduction of global carbon emissions. It provides a solution for storing and managing the intermittency of renewable energy sources, enabling more consistent and efficient use of these resources. As an energy carrier, hydrogen can be generated from various renewable sources, making it adaptable and suitable for diverse energy scenarios. Moreover, its use reduces greenhouse gas emissions, a crucial factor in combating climate change. This research stands out from other global studies in several aspects. For example, Zhang et al. [48] conducted a study on the optimal sizing of an autonomous hybrid system combining solar, wind, and hydrogen, using weather forecasts and a hybrid search algorithm. However, they did not apply their research to a local context in sub-Saharan Africa, considering the specific seasonal climatic conditions and the energy needs of rural communities. The study by Torreglosa et al. [52] on a hybrid renewable energy system based on a wind fuel cell/electrolyzer does not focus on a remote region as this study does, which adds a dimension of specific local and climatic adaptation not present in their work. This study specifically targets agricultural and rural communities in sub-Saharan Africa with a practical approach to rural electrification. Unlike Pablo et al. [50], who studied the performance of a hybrid system to meet the energy demand of a livestock facility using renewable energy sources, this study is distinguished by its unique application context in a remote region of sub-Saharan Africa. It integrates local seasonal climatic variables and aims to meet the specific needs of rural and agricultural communities. Instead of following the approaches mentioned in previous studies, this research focuses on adapting energy solutions to African conditions. Offering a fresh perspective could potentially facilitate the broader adoption of this technology in similar regions.

In the scientific literature, several studies have conducted sensitivity analyses, including those by [53], [54], [55], and [59], although these studies present certain limitations. Alonso et al. [53] evaluated various energy storage technologies in Belgium, considering different energy scenarios such as consumption, electricity tariffs, CO_2 taxation, and the evolution of hydrogen technology prices from 2019 to 2030. Turkdogan et al. [54]conducted a sensitivity analysis on the cost of electricity and hydrogen in relation to the reduction in the costs of electrolyzers, photovoltaic panels, and wind turbines. Basu et al. [55] studied three combinations of energy systems in India, focusing on the current cost of energy (LCOE), capital expenditures (CAPEX), and operational expenditures (OPEX). Finally, Askarzadeh et al. [59] explored the optimal sizing and power exchange of a diesel-photovoltaic-fuel cell hybrid system in Iran, focusing on sale and purchase coefficients as well as the variation in the use of non-renewable energy sources.

The second innovation of this research lies in its specific application to the sub-Saharan context, integrating local climatic conditions and the energy needs of rural and agricultural communities. Unlike other studies that mainly focus on urban or industrial contexts, this research examines the effects of variations in wind speed and solar radiation on the cost of energy. It also demonstrates that increased wind speed and solar radiation significantly reduce the cost of energy. It highlights the impact of capacity shortage tolerance on the total current cost and the cost of energy, showing that a certain tolerance (up to 5%) can minimize costs without significantly affecting system reliability. The study also illustrates the effect of variations in capital expenditures and replacement costs of photovoltaic systems and fuel cells on the optimal configuration of the hybrid system.

In this context, sensitivity analysis is crucial because it helps identify the most cost-effective and efficient energy system configurations, tailored to the specific conditions of sub-Saharan Africa. It also allows for the modeling and optimization of climate-based energy systems by taking local conditions into account, such as seasonal variations in wind speed and solar radiation. This facilitates the design of robust and reliable energy systems for rural areas, where access to electricity is limited, and fossil resources are often inaccessible or expensive. Sensitivity analysis contributes to minimizing

Preprints.org (www.preprints.org) | NOT PEER-REVIEWED | Posted: 25 December 2024 doi:10.20944/preprints202412.2206.v1

energy costs by optimizing investments, making renewable energy solutions more accessible and sustainable for rural communities. By improving access to reliable and affordable energy, this analysis supports local economic development, reduces dependence on fossil fuels, and promotes more sustainable agricultural practices.

The introduction of electricity into a remote community like Dargalla transforms the daily lives of its residents. This project has had significant impacts on several aspects. In terms of economic development and health, electrification has encouraged the emergence of small businesses and income-generating activities such as sewing, welding, and the preservation of agricultural products [96]. It has also increased agricultural productivity through the use of electrical equipment for irrigation and post-harvest processing [97]. Additionally, the transition from kerosene to electric lighting has reduced indoor air pollution, contributing to a decrease in respiratory diseases [98]. Agriculture is a major pillar of the rural economy in sub-Saharan Africa, and access to electricity is vital for agricultural activities. However, the lack of energy has been identified as the main obstacle to the productivity of the agricultural sector in sub-Saharan Africa, where only 2% of the final electricity consumption is dedicated to agriculture, compared to 18% in India [99]. This initiative will also play a role in improving study conditions by providing better lighting for students, thus extending study hours and improving academic performance [100]. Furthermore, it will facilitate access to information and educational resources through information and communication technologies [101].

The electrification of Dargalla, a rural hamlet in sub-Saharan Africa, through hybrid systems with hydrogen storage presents notable advantages but also faces several hurdles. Overcoming these obstacles is crucial to ensure the success and sustainability of such projects. The installation of complex systems like hybrid microgrids, which require sophisticated integration of various energy sources and storage technologies (such as hydrogen), can present challenges in terms of maintenance and technical management [102]. Additionally, the lack of appropriate policies and regulatory frameworks to support renewable energies and hydrogen storage technologies hinders the development and installation of these systems [103]. The absence of adequate infrastructure to support the installation, operation, and maintenance of hydrogen storage systems and hybrid systems makes their implementation in remote areas difficult [104]. Finally, the lack of sufficient funding and viable economic models for hydrogen storage projects in rural areas impedes their large-scale adoption [105].

To address the limitations of this study, further research could focus on the long-term sustainability of hybrid systems with hydrogen storage, including the evaluation of component degradation and maintenance requirements over several years. Additional studies could also consider viable economic models and financing strategies to make hydrogen storage projects more accessible and sustainable in rural areas. This could highlight opportunities and challenges for the adoption of these technologies. It would also be relevant to compare the efficiency and economic viability of hybrid systems with hydrogen storage to other storage solutions such as batteries or pumped hydroelectric storage.

5. Conclusions

This study proposes an innovative and pragmatic solution for the electrification of rural areas in sub-Saharan Africa using hybrid energy systems integrating photovoltaic, wind, and hydrogen storage. The results show that this configuration can reliably and economically meet the energy needs of rural communities while minimizing environmental impact. The integration of hydrogen storage proves particularly effective in overcoming the challenges of renewable source intermittency, ensuring a continuous energy supply. The thorough sensitivity analysis demonstrated that variations in wind speed and solar radiation significantly influence the cost of energy, highlighting the importance of local adaptation of energy systems. By combining precise modeling of local energy needs with the optimization of renewable resources, this study provides a robust framework for the development of sustainable energy solutions. The proposed approach not only improves access to electricity but also promotes economic and social development by stimulating income-generating activities and improving living conditions. To go further, additional studies on long-term sustainability, financing strategies, and integration of energy policies are necessary to maximize the impact and viability of these hybrid systems. These research efforts will help refine existing models and propose even more resilient solutions to global energy challenges.

References

1. Löfquist, L. Is There a Universal Human Right to Electricity? *The International Journal of Human Rights* **2020**, *24*, 711–723, doi:10.1080/13642987.2019.1671355.
2. Mukhtar, M.; Ameyaw, B.; Yimen, N.; Zhang, Q.; Bamisile, O.; Adun, H.; Dagbasi, M. Building Retrofit and Energy Conservation/Efficiency Review: A Techno-Environ-Economic Assessment of Heat Pump System Retrofit in Housing Stock. *Sustainability* **2021**, *13*, 983.
3. Bamisile, O.; Mukhtar, M.; Yimen, N.; Huang, Q.; Olotu, O.; Adebayo, V.; Dagabsi, M. Comparative Performance Analysis of Solar Powered Supercritical-Transcritical CO2 Based Systems for Hydrogen Production and Multigeneration. *International Journal of Hydrogen Energy* **2021**, *46*, 26272–26288.
4. Bamisile, O.; Oluwasanmi, A.; Ejiyi, C.; Yimen, N.; Obiora, S.; Huang, Q. Comparison of Machine Learning and Deep Learning Algorithms for Hourly Global/Diffuse Solar Radiation Predictions. *Intl J of Energy Research* **2022**, *46*, 10052–10073, doi:10.1002/er.6529.
5. Mukhtar, M.; Oluwasanmi, A.; Yimen, N.; Qinxiu, Z.; Ukwuoma, C.C.; Ezurike, B.; Bamisile, O. Development and Comparison of Two Novel Hybrid Neural Network Models for Hourly Solar Radiation Prediction. *Applied Sciences* **2022**, *12*, 1435.
6. Mukhtar, M.; Obiora, S.; Yimen, N.; Quixin, Z.; Bamisile, O.; Jidele, P.; Irivboje, Y.I. Effect of Inadequate Electrification on Nigeria's Economic Development and Environmental Sustainability. *Sustainability* **2021**, *13*, 2229.
7. Yimen, N.; Dagbasi, M. Multi-Attribute Decision-Making: Applying a Modified Brown–Gibson Model and RETScreen Software to the Optimal Location Process of Utility-Scale Photovoltaic Plants. *Processes* **2019**, *7*, 505.
8. Kober, T.; Schiffer, H.-W.; Densing, M.; Panos, E. Global Energy Perspectives to 2060–WEC's World Energy Scenarios 2019. *Energy Strategy Reviews* **2020**, *31*, 100523.
9. Ritchie, H.; Rosado, P.; Roser, M. Access to Energy. *Our World in Data* **2024**.
10. Sarkodie, S.A.; Adams, S. Electricity Access and Income Inequality in South Africa: Evidence from Bayesian and NARDL Analyses. *Energy Strategy Reviews* **2020**, *29*, 100480.
11. Ritchie, H.; Rosado, P.; Roser, M. Access to Energy. *Our World in Data* **2024**.
12. Bamisile, O.; Ojo, O.; Yimen, N.; Adun, H.; Li, J.; Obiora, S.; Huang, Q. Comprehensive Functional Data Analysis of China's Dynamic Energy Security Index. *Energy Reports* **2021**, *7*, 6246–6259.
13. Zigah, E.; Creti, A. A Comparative Analysis of Electricity Access Initiatives in Sub-Saharan Africa. In *Regional Approaches to the Energy Transition*; Gromek-Broc, K., Ed.; Springer International Publishing: Cham, 2023; pp. 271–306 ISBN 978-3-031-19357-6.
14. Ouedraogo, N.S. A GIS Approach to Electrification Planning in Cameroon. *Energy Strategy Reviews* **2023**, *45*, 101020.
15. Musa, B.; Yimen, N.; Abba, S.I.; Adun, H.H.; Dagbasi, M. Multi-State Load Demand Forecasting Using Hybridized Support Vector Regression Integrated with Optimal Design of off-Grid Energy Systems—A Metaheuristic Approach. *Processes* **2021**, *9*, 1166.
16. Abba, S.I.; Rotimi, A.; Musa, B.; Yimen, N.; Kawu, S.J.; Lawan, S.M.; Dagbasi, M. Emerging Harris Hawks Optimization Based Load Demand Forecasting and Optimal Sizing of Stand-Alone Hybrid Renewable Energy Systems–A Case Study of Kano and Abuja, Nigeria. *Results in Engineering* **2021**, *12*, 100260.

17. Biboum, A.; Yilanci, A.; Olivier Thierry, S.M.; Yimen, N.; Mouangue, R. Investigation of Concentrating Solar-Biomass-Fired Power Technologies Based on Advanced Exergy, Exergoeconomic and Exergoenvironmental Analyses. *Energy Sources, Part A: Recovery, Utilization, and Environmental Effects* **2023**, *45*, 9668–9683, doi:10.1080/15567036.2023.2239747.
18. Yimen, N.; Monkam, L.; Tcheukam-Toko, D.; Musa, B.; Abang, R.; Fombe, L.F.; Abbasoglu, S.; Dagbasi, M. Optimal Design and Sensitivity Analysis of Distributed Biomass-based Hybrid Renewable Energy Systems for Rural Electrification: Case Study of Different Photovoltaic/Wind/Battery-integrated Options in Babadam, Northern Cameroon. *IET Renewable Power Gen* **2022**, *16*, 2939–2956, doi:10.1049/rpg2.12266.
19. Adaramola, M.S.; Agelin-Chaab, M.; Paul, S.S. Analysis of Hybrid Energy Systems for Application in Southern Ghana. *Energy Conversion and Management* **2014**, *88*, 284–295, doi:10.1016/j.enconman.2014.08.029.
20. Nfah, E.M.; Ngundam, J.M. Feasibility of Pico-Hydro and Photovoltaic Hybrid Power Systems for Remote Villages in Cameroon. *Renewable Energy* **2009**, *34*, 1445–1450, doi:10.1016/j.renene.2008.10.019.
21. Baghdadi, F.; Mohammedi, K.; Diaf, S.; Behar, O. Feasibility Study and Energy Conversion Analysis of Stand-Alone Hybrid Renewable Energy System. *Energy Conversion and Management* **2015**, *105*, 471–479, doi:10.1016/j.enconman.2015.07.051.
22. Singh, S.; Singh, M.; Kaushik, S.C. Feasibility Study of an Islanded Microgrid in Rural Area Consisting of PV, Wind, Biomass and Battery Energy Storage System. *Energy Conversion and Management* **2016**, *128*, 178–190, doi:10.1016/j.enconman.2016.09.046.
23. Ghaem Sigarchian, S.; Paleta, R.; Malmquist, A.; Pina, A. Feasibility Study of Using a Biogas Engine as Backup in a Decentralized Hybrid (PV/Wind/Battery) Power Generation System – Case Study Kenya. *Energy* **2015**, *90*, 1830–1841, doi:10.1016/j.energy.2015.07.008.
24. Kenfack, J.; Neirac, F.P.; Tatietse, T.T.; Mayer, D.; Fogue, M.; Lejeune, A. Microhydro-PV-Hybrid System: Sizing a Small Hydro-PV-Hybrid System for Rural Electrification in Developing Countries. *Renewable Energy* **2009**, *34*, 2259–2263, doi:10.1016/j.renene.2008.12.038.
25. Sanajaoba Singh, S.; Fernandez, E. Modeling, Size Optimization and Sensitivity Analysis of a Remote Hybrid Renewable Energy System. *Energy* **2018**, *143*, 719–731, doi:10.1016/j.energy.2017.11.053.
26. Halabi, L.M.; Mekhilef, S.; Olatomiwa, L.; Hazelton, J. Performance Analysis of Hybrid PV/Diesel/Battery System Using HOMER: A Case Study Sabah, Malaysia. *Energy Conversion and Management* **2017**, *144*, 322–339, doi:10.1016/j.enconman.2017.04.070.
27. Bhakta, S.; Mukherjee, V. Performance Indices Evaluation and Techno Economic Analysis of Photovoltaic Power Plant for the Application of Isolated India's Island. *Sustainable Energy Technologies and Assessments* **2017**, *20*, 9–24, doi:10.1016/j.seta.2017.02.002.
28. Sawle, Y.; Gupta, S.C.; Bohre, A.K. Socio-Techno-Economic Design of Hybrid Renewable Energy System Using Optimization Techniques. *Renewable Energy* **2018**, *119*, 459–472, doi:10.1016/j.renene.2017.11.058.
29. Singh, N.K.; Koley, C.; Gope, S.; Dawn, S.; Ustun, T.S. An Economic Risk Analysis in Wind and Pumped Hydro Energy Storage Integrated Power System Using Meta-Heuristic Algorithm. *Sustainability* **2021**, *13*.
30. Petrollese, M.; Seche, P.; Cocco, D. Analysis and Optimization of Solar-Pumped Hydro Storage Systems Integrated in Water Supply Networks. *Energy* **2019**, *189*, 116176, doi:10.1016/j.energy.2019.116176.
31. Ali, S.; Stewart, R.A.; Sahin, O. Drivers and Barriers to the Deployment of Pumped Hydro Energy Storage Applications: Systematic Literature Review. *Cleaner Engineering and Technology* **2021**, *5*, 100281, doi:10.1016/j.clet.2021.100281.
32. Nassar, Y.F.; Abdunnabi, M.J.; Sbeta, M.N.; Hafez, A.A.; Amer, K.A.; Ahmed, A.Y.; Belgasim, B. Dynamic Analysis and Sizing Optimization of a Pumped Hydroelectric Storage-Integrated Hybrid PV/Wind System: A Case Study. *Energy Conversion and Management* **2021**, *229*, 113744, doi:10.1016/j.enconman.2020.113744.

33. Ko, Y.; Choi, G.; Lee, S.; Kim, S. Economic Analysis of Pumped Hydro Storage under Korean Governmental Expansion Plan for Renewable Energy. *Energy Reports* **2020**, *6*, 214–220, doi:10.1016/j.egyr.2019.08.047.
34. Ayodele, T.R.; Ogunjuyigbe, A.S.O.; Ibitoye, T.Y. Optimal Selection of Pumped Hydro Storage Based Renewable Energy Generator(s) for Isolated Community Using Binary Sort and Search Algorithm. *Renewable Energy Focus* **2019**, *28*, 100–111, doi:10.1016/j.ref.2018.12.003.
35. Segurado, R.; Madeira, J.F.A.; Costa, M.; Duić, N.; Carvalho, M.G. Optimization of a Wind Powered Desalination and Pumped Hydro Storage System. *Applied Energy* **2016**, *177*, 487–499, doi:10.1016/j.apenergy.2016.05.125.
36. Kusakana, K. Optimization of the Daily Operation of a Hydrokinetic–Diesel Hybrid System with Pumped Hydro Storage. *Energy Conversion and Management* **2015**, *106*, 901–910, doi:10.1016/j.enconman.2015.10.021.
37. Makhdoomi, S.; Askarzadeh, A. Optimizing Operation of a Photovoltaic/Diesel Generator Hybrid Energy System with Pumped Hydro Storage by a Modified Crow Search Algorithm. *Journal of Energy Storage* **2020**, *27*, 101040, doi:10.1016/j.est.2019.101040.
38. Bhayo, B.A.; Al-Kayiem, H.H.; Gilani, S.I.U.; Ismail, F.B. Power Management Optimization of Hybrid Solar Photovoltaic-Battery Integrated with Pumped-Hydro-Storage System for Standalone Electricity Generation. *Energy Conversion and Management* **2020**, *215*, 112942, doi:10.1016/j.enconman.2020.112942.
39. Rehman, S.; Al-Hadhrami, L.M.; Alam, Md.M. Pumped Hydro Energy Storage System: A Technological Review. *Renewable and Sustainable Energy Reviews* **2015**, *44*, 586–598, doi:10.1016/j.rser.2014.12.040.
40. Maleki, A.; Askarzadeh, A. Comparative Study of Artificial Intelligence Techniques for Sizing of a Hydrogen-Based Stand-Alone Photovoltaic/Wind Hybrid System. *International Journal of Hydrogen Energy* **2014**, *39*, 9973–9984, doi:10.1016/j.ijhydene.2014.04.147.
41. Hunt, J.D.; Falchetta, G.; Parkinson, S.; Vinca, A.; Zakeri, B.; Byers, E.; Jurasz, J.; Quaranta, E.; Grenier, E.; Junior, A.O.P. Hydropower and Seasonal Pumped Hydropower Storage in the Indus Basin: Pros and Cons. *Journal of Energy Storage* **2021**, *41*, 102916.
42. Bamisile, O.; Babatunde, A.; Adun, H.; Yimen, N.; Mukhtar, M.; Huang, Q.; Hu, W. Electrification and Renewable Energy Nexus in Developing Countries; an Overarching Analysis of Hydrogen Production and Electric Vehicles Integrality in Renewable Energy Penetration. *Energy Conversion and Management* **2021**, *236*, 114023.
43. Bamisile, O.; Obiora, S.; Huang, Q.; Yimen, N.; Idriss, I.A.; Cai, D.; Dagbasi, M. Impact of Economic Development on CO2 Emission in Africa; the Role of BEVs and Hydrogen Production in Renewable Energy Integration. *International Journal of Hydrogen Energy* **2021**, *46*, 2755–2773.
44. Mukhtar, M.; Adebayo, V.; Yimen, N.; Bamisile, O.; Osei-Mensah, E.; Adun, H.; Zhang, Q.; Luo, G. Towards Global Cleaner Energy and Hydrogen Production: A Review and Application ORC Integrality with Multigeneration Systems. *Sustainability* **2022**, *14*, 5415.
45. Peng, T.; Wan, J.; Liu, W.; Li, J.; Xia, Y.; Yuan, G.; Jurado, M.J.; Fu, P.; He, Y.; Liu, H. Choice of Hydrogen Energy Storage in Salt Caverns and Horizontal Cavern Construction Technology. *Journal of Energy Storage* **2023**, *60*, 106489.
46. Arsad, A.Z.; Hannan, M.; Al-Shetwi, A.Q.; Mansur, M.; Muttaqi, K.; Dong, Z.; Blaabjerg, F. Hydrogen Energy Storage Integrated Hybrid Renewable Energy Systems: A Review Analysis for Future Research Directions. *International Journal of Hydrogen Energy* **2022**, *47*, 17285–17312.
47. Klumpp, F. Comparison of Pumped Hydro, Hydrogen Storage and Compressed Air Energy Storage for Integrating High Shares of Renewable Energies—Potential, Cost-Comparison and Ranking. *Journal of Energy storage* **2016**, *8*, 119–128.

Preprints.org (www.preprints.org) | NOT PEER-REVIEWED | Posted: 25 December 2024 doi:10.20944/preprints202412.2206.v1

48. Zhang, W.; Maleki, A.; Rosen, M.A.; Liu, J. Sizing a Stand-Alone Solar-Wind-Hydrogen Energy System Using Weather Forecasting and a Hybrid Search Optimization Algorithm. *Energy Conversion and Management* **2019**, *180*, 609–621, doi:10.1016/j.enconman.2018.08.102.
49. Dufo-López, R.; Bernal-Agustín, J.L.; Mendoza, F. Design and Economical Analysis of Hybrid PV–Wind Systems Connected to the Grid for the Intermittent Production of Hydrogen. *Energy Policy* **2009**, *37*, 3082–3095, doi:10.1016/j.enpol.2009.03.059.
50. García, P.; Torreglosa, J.P.; Fernández, L.M.; Jurado, F. Optimal Energy Management System for Stand-Alone Wind Turbine/Photovoltaic/Hydrogen/Battery Hybrid System with Supervisory Control Based on Fuzzy Logic. *International Journal of Hydrogen Energy* **2013**, *38*, 14146–14158, doi:10.1016/j.ijhydene.2013.08.106.
51. Akyuz, E.; Oktay, Z.; Dincer, I. Performance Investigation of Hydrogen Production from a Hybrid Wind-PV System. *International Journal of Hydrogen Energy* **2012**, *37*, 16623–16630, doi:10.1016/j.ijhydene.2012.02.149.
52. Torreglosa, J.P.; García, P.; Fernández, L.M.; Jurado, F. Energy Dispatching Based on Predictive Controller of an Off-Grid Wind Turbine/Photovoltaic/Hydrogen/Battery Hybrid System. *Renewable Energy* **2015**, *74*, 326–336, doi:10.1016/j.renene.2014.08.010.
53. Alonso, A.M.; Costa, D.; Messagie, M.; Coosemans, T. Techno-Economic Assessment on Hybrid Energy Storage Systems Comprising Hydrogen and Batteries: A Case Study in Belgium. *International Journal of Hydrogen Energy* **2024**, *52*, 1124–1135, doi:10.1016/j.ijhydene.2023.06.282.
54. Turkdogan, S. Design and Optimization of a Solely Renewable Based Hybrid Energy System for Residential Electrical Load and Fuel Cell Electric Vehicle. *Engineering Science and Technology, an International Journal* **2021**, *24*, 397–404, doi:10.1016/j.jestch.2020.08.017.
55. Basu, S.; John, A.; Akshay; Kumar, A. Design and Feasibility Analysis of Hydrogen Based Hybrid Energy System: A Case Study. *International Journal of Hydrogen Energy* **2021**, *46*, 34574–34586, doi:10.1016/j.ijhydene.2021.08.036.
56. Hosseinalizadeh, R.; Shakouri G, H.; Amalnick, M.S.; Taghipour, P. Economic Sizing of a Hybrid (PV–WT–FC) Renewable Energy System (HRES) for Stand-Alone Usages by an Optimization-Simulation Model: Case Study of Iran. *Renewable and Sustainable Energy Reviews* **2016**, *54*, 139–150, doi:10.1016/j.rser.2015.09.046.
57. Jahangir, M.H.; Javanshir, F.; Kargarzadeh, A. Economic Analysis and Optimal Design of Hydrogen/Diesel Backup System to Improve Energy Hubs Providing the Demands of Sport Complexes. *International Journal of Hydrogen Energy* **2021**, *46*, 14109–14129, doi:10.1016/j.ijhydene.2021.01.187.
58. Dufo-López, R.; Bernal-Agustín, J.L. Multi-Objective Design of PV–Wind–Diesel–Hydrogen–Battery Systems. *Renewable Energy* **2008**, *33*, 2559–2572, doi:10.1016/j.renene.2008.02.027.
59. Gharibi, M.; Askarzadeh, A. Size and Power Exchange Optimization of a Grid-Connected Diesel Generator-Photovoltaic-Fuel Cell Hybrid Energy System Considering Reliability, Cost and Renewability. *International Journal of Hydrogen Energy* **2019**, *44*, 25428–25441, doi:10.1016/j.ijhydene.2019.08.007.
60. Caliskan, A.; Percin, H.B. Techno-Economic Analysis of a Campus-Based Hydrogen-Producing Hybrid System. *International Journal of Hydrogen Energy* **2024**, *75*, 428–437, doi:10.1016/j.ijhydene.2024.02.140.
61. Amuakwa-Mensah, S.; Surry, Y. Association between Rural Electrification and Agricultural Output: Evidence from Sub-Saharan Africa. *World Development Perspectives* **2022**, *25*, 100392, doi:10.1016/j.wdp.2021.100392.
62. Sinha, S.; Chandel, S.S. Review of Software Tools for Hybrid Renewable Energy Systems. *Renewable and Sustainable Energy Reviews* **2014**, *32*, 192–205, doi:10.1016/j.rser.2014.01.035.
63. Kavadias, K.A.; Triantafyllou, P. Hybrid Renewable Energy Systems' Optimisation. A Review and Extended Comparison of the Most-Used Software Tools. *Energies* **2021**, *14*, 8268, doi:10.3390/en14248268.

64. Shaikh, P.H.; Shaikh, A.; Memon, Z.A.; Lashari, A.A.; Leghari, Z.H. Microgrids: A Review on Optimal Hybrid Technologies, Configurations, and Applications. *International Journal of Energy Research* **2021**, *45*, 12564–12597, doi:10.1002/er.6666.
65. Jahangir, M.H.; Javanshir, F.; Kargarzadeh, A. Economic Analysis and Optimal Design of Hydrogen/Diesel Backup System to Improve Energy Hubs Providing the Demands of Sport Complexes. *International Journal of Hydrogen Energy* **2021**, *46*, 14109–14129, doi:10.1016/j.ijhydene.2021.01.187.
66. TSUANYO, D.B. Approches Technico-Économiques d'optimisation Des Systèmes Énergétiques Décentralisés: Cas Des Systèmes Hybrides PV/Diesel. PhD Thesis, UNIVERSITE DE PERPIGNAN VIA DOMITIA, 2015.
67. Yimen, N.; Hamandjoda, O.; Meva'a, L.; Ndzana, B.; Nganhou, J. Analyzing of a Photovoltaic/Wind/Biogas/Pumped-Hydro Off-Grid Hybrid System for Rural Electrification in Sub-Saharan Africa—Case Study of Djoundé in Northern Cameroon. *Energies* **2018**, *11*, 1–30.
68. Mwammenywa, I.; Hilleringmann, U. Analysis of Electricity Power Generation and Load Profiles in Solar PV Microgrids in Rural Villages of East Africa: Case of Mpale Village in Tanzania. In Proceedings of the 2023 IEEE AFRICON; September 2023; pp. 1–6.
69. Williams, N.J.; Jaramillo, P.; Campbell, K.; Musanga, B.; Lyons-Galante, I. Electricity Consumption and Load Profile Segmentation Analysis for Rural Micro Grid Customers in Tanzania. In Proceedings of the 2018 IEEE PES/IAS PowerAfrica; June 2018; pp. 360–365.
70. NASA POWER | Prediction Of Worldwide Energy Resources Available online: https://power.larc.nasa.gov/ (accessed on 6 July 2023).
71. Prodromidis, G.N.; Coutelieris, F.A. Simulation and Optimization of a Stand-Alone Power Plant Based on Renewable Energy Sources. *International Journal of Hydrogen Energy* **2010**, *35*, 10599–10603, doi:10.1016/j.ijhydene.2010.07.065.
72. Okundamiya, M.S. Size Optimization of a Hybrid Photovoltaic/Fuel Cell Grid Connected Power System Including Hydrogen Storage. *International Journal of Hydrogen Energy* **2021**, *46*, 30539–30546, doi:10.1016/j.ijhydene.2020.11.185.
73. Sunpower SPR-E20-327-C-AC (327W) Solar Panel Available online: http://www.solardesigntool.com/components/module-panel-solar/Sunpower/3228/SPR-E20-327-C-AC/specification-data-sheet.html (accessed on 22 July 2024).
74. Luta, D.N.; Raji, A.K. Decision-Making between a Grid Extension and a Rural Renewable off-Grid System with Hydrogen Generation. *International Journal of Hydrogen Energy* **2018**, *43*, 9535–9548, doi:10.1016/j.ijhydene.2018.04.032.
75. Yimen, N.; Tchotang, T.; Kanmogne, A.; Abdelkhalikh Idriss, I.; Musa, B.; Aliyu, A.; Okonkwo, E.C.; Abba, S.I.; Tata, D.; Meva'a, L.; et al. Optimal Sizing and Techno-Economic Analysis of Hybrid Renewable Energy Systems—A Case Study of a Photovoltaic/Wind/Battery/Diesel System in Fanisau, Northern Nigeria. *Processes* **2020**, *8*, 1381, doi:10.3390/pr8111381.
76. Excel 10 Off Grid. *Bergey Windpower Co.*
77. Abdelkareem, M.A.; Elsaid, K.; Wilberforce, T.; Kamil, M.; Sayed, E.T.; Olabi, A. Environmental Aspects of Fuel Cells: A Review. *Science of The Total Environment* **2021**, *752*, 141803, doi:10.1016/j.scitotenv.2020.141803.
78. Chitsaz, A.; Haghghi, M.A.; Hosseinpour, J. Thermodynamic and Exergoeconomic Analyses of a Proton Exchange Membrane Fuel Cell (PEMFC) System and the Feasibility Evaluation of Integrating with a Proton Exchange Membrane Electrolyzer (PEME). *Energy Conversion and Management* **2019**, *186*, 487–499, doi:10.1016/j.enconman.2019.03.004.

79. Amores, E.; Sánchez, M.; Rojas, N.; Sánchez-Molina, M. 9 - Renewable Hydrogen Production by Water Electrolysis. In *Sustainable Fuel Technologies Handbook*; Dutta, S., Mustansar Hussain, C., Eds.; Academic Press, 2021; pp. 271–313 ISBN 978-0-12-822989-7.
80. Smolinka, T. FUELS – HYDROGEN PRODUCTION | Water Electrolysis. In *Encyclopedia of Electrochemical Power Sources*; Garche, J., Ed.; Elsevier: Amsterdam, 2009; pp. 394–413 ISBN 978-0-444-52745-5.
81. Paul, B.; Andrews, J. Optimal Coupling of PV Arrays to PEM Electrolysers in Solar–Hydrogen Systems for Remote Area Power Supply. *International Journal of Hydrogen Energy* **2008**, *33*, 490–498, doi:10.1016/j.ijhydene.2007.10.040.
82. Roger, M.B.T.; Théodore, T.; Nasser, Y.; Augustin, E.N.A.; Ornella, K.D.G. Integrating Hydrogen into a Hybrid System to Meet a Laboratory's Electricity Demand. *International Journal of Hydrogen Energy* **2024**, *87*, 736–756.
83. Pal, P.; Mukherjee, V. Off-Grid Solar Photovoltaic/Hydrogen Fuel Cell System for Renewable Energy Generation: An Investigation Based on Techno-Economic Feasibility Assessment for the Application of End-User Load Demand in North-East India. *Renewable and Sustainable Energy Reviews* **2021**, *149*, 111421, doi:10.1016/j.rser.2021.111421.
84. Uwineza, L.; Kim, H.-G.; Kleissl, J.; Kim, C.K. Technical Control and Optimal Dispatch Strategy for a Hybrid Energy System. *Energies* **2022**, *15*, 2744, doi:10.3390/en15082744.
85. WILLIAMSON, L.E.; CONNOR, H.; MOEZZI, M. Climatiser Les Systèmes Énergétiques. **2009**.
86. Ochieng, F.X. Application of Grid Computing for Meteorological Assessment of Wind and Solar Resources in Sub-Saharan African Countries. In *Computational and Data Grids: Principles, Applications and Design*; IGI Global, 2012; pp. 283–290 ISBN 978-1-61350-113-9.
87. Upreti, G.; Greene, D.L.; Duleep, K.G.; Sawhney, R. Fuel Cells for Non-Automotive Uses: Status and Prospects. *International Journal of Hydrogen Energy* **2012**, *37*, 6339–6348, doi:10.1016/j.ijhydene.2012.01.060.
88. Ren, X.; Lv, Q.; Liu, L.; Liu, B.; Wang, Y.; Liu, A.; Wu, G. Current Progress of Pt and Pt-Based Electrocatalysts Used for Fuel Cells. *Sustainable Energy Fuels* **2020**, *4*, 15–30, doi:10.1039/C9SE00460B.
89. Current and Future Cost of Photovoltaics Available online: https://www.agora-energiewende.org/publications/current-and-future-cost-of-photovoltaics (accessed on 14 June 2024).
90. Falama, R.Z.; Dumbrava, V.; Saidi, A.S.; Houdji, E.T.; Salah, C.B.; Doka, S.Y. A Comparative-Analysis-Based Multi-Criteria Assessment of On/Off-Grid-Connected Renewable Energy Systems: A Case Study. *Energies* **2023**, *16*, 1540, doi:10.3390/en16031540.
91. Jahangiri, M.; Soulouknga, M.H.; Bardei, F.K.; Shamsabadi, A.A.; Akinlabi, E.T.; Sichilalu, S.M.; Mostafaeipour, A. Techno-Econo-Environmental Optimal Operation of Grid-Wind-Solar Electricity Generation with Hydrogen Storage System for Domestic Scale, Case Study in Chad. *International Journal of Hydrogen Energy* **2019**, *44*, 28613–28628, doi:10.1016/j.ijhydene.2019.09.130.
92. Barasa, M.; Bogdanov, D.; Oyewo, A.S.; Breyer, C. A Cost Optimal Resolution for Sub-Saharan Africa Powered by 100% Renewables in 2030. *Renewable and Sustainable Energy Reviews* **2018**, *92*, 440–457, doi:10.1016/j.rser.2018.04.110.
93. Mbaka, N.E.; Mucho, N.J.; Godpromesse, K. Economic Evaluation of Small-Scale Photovoltaic Hybrid Systems for Mini-Grid Applications in Far North Cameroon. *Renewable Energy* **2010**, *35*, 2391–2398, doi:10.1016/j.renene.2010.03.005.
94. Muh, E.; Tabet, F. Comparative Analysis of Hybrid Renewable Energy Systems for Off-Grid Applications in Southern Cameroons. *Renewable Energy* **2019**, *135*, 41–54, doi:10.1016/j.renene.2018.11.105.

95. Adaramola, M.S.; Oyewola, O.M.; Paul, S.S. Technical and Economic Assessment of Hybrid Energy Systems in South-West Nigeria. *Energy Exploration & Exploitation* **2012**, *30*, 533–551, doi:10.1260/0144-5987.30.4.533.
96. Khandker, S.; Barnes, D.; Samad, H. Welfare Impacts of Rural Electrification: A Panel Data Analysis from Vietnam. *Economic Development and Cultural Change* **2013**, *61*, 659–692, doi:10.1086/669262.
97. Dinkelman, T. The Effects of Rural Electrification on Employment: New Evidence from South Africa. *American Economic Review* **2011**, *101*, 3078–3108, doi:10.1257/aer.101.7.3078.
98. Barron, M.; Torero, M. Household Electrification and Indoor Air Pollution. *Journal of Environmental Economics and Management* **2017**, *86*, 81–92, doi:10.1016/j.jeem.2017.07.007.
99. Https://Www.Iea.Org/Publications/Freepublications/Publication/WEO2017SpecialReport_EnergyAccessOutlook.Pdf Available online: https://www.iea.org/publications/freepublications/publication/WEO2017SpecialReport_EnergyAccessOutlook.pdf (accessed on 20 June 2024).
100. Grimm, R.; Fox, C.; Baines, S.; Albertson, K. Social Innovation, an Answer to Contemporary Societal Challenges? Locating the Concept in Theory and Practice. *Innovation: The European Journal of Social Science Research*, **2013**, *26*, 463–455, doi:10.1080/13511610.2013.848163.
101. Peters, J.; Strupat, C.; Vance, C. Television and Contraceptive Use - A Weak Signal? *Journal of Development Studies* **2014**, *50*, 1538–1549.
102. Baldinelli, A.; Barelli, L.; Bidini, G. Sustainable Water-Energy Innovations for Higher Comfort of Living in Remote and Rural Areas from Developing Countries: From Seawater to Hydrogen through Reversible Solid Oxide Cells. *Journal of Cleaner Production* **2021**, *321*, 128846, doi:10.1016/j.jclepro.2021.128846.
103. Moner-Girona, M.; Solano-Peralta, M.; Lazopoulou, M.; Ackom, E.K.; Vallve, X.; Szabó, S. Electrification of Sub-Saharan Africa through PV/Hybrid Mini-Grids: Reducing the Gap between Current Business Models and on-Site Experience. *Renewable and Sustainable Energy Reviews* **2018**, *91*, 1148–1161, doi:10.1016/j.rser.2018.04.018.
104. Fopah-Lele, A. Hydrogen Technology in Sub-Saharan Africa: Prospects for Power Plants. *E3S Web Conf.* **2022**, *354*, 01001, doi:10.1051/e3sconf/202235401001.
105. Mandelli, S.; Brivio, C.; Leonardi, M.; Colombo, E.; Molinas, M.; Park, E.; Merlo, M. The Role of Electrical Energy Storage in Sub-Saharan Africa. *Journal of Energy Storage* **2016**, *8*, 287–299, doi:10.1016/j.est.2015.11.006.